Dear Editors and Reviewers

Thank you for your time in reviewing our submission. We are grateful for the opportunity to respond to the reviewer's comments, which have proven extremely useful in revising this manuscript. We have now revised the manuscript offering additional information and context.

Below you will find a detailed response to each comment presented by the reviewers and how these changes are incorporated in the revised manuscript.

Yours sincerely

Geoffrey Dawson

REVIEWER 1

1) The methodology adopted requires a 3 year moving window hence limiting the ability of capturing grounding line dynamic nonlinear retreats.

The main purpose of this study was to map the grounding zone and not to capture grounding line dynamic nonlinear retreats. However, it is correct that the method presented here cannot capture these events, and we have now included this as a limitation (line 100).

2) The author claims this method could potentially monitor retreat in the Amundsen Sea mbayment (ASE). They also claim no significant changes in grounding line position were detected over the ASE in the period 2010-2017. This contrasts with DInSAR measurements performed during the same period (See Milillo et al 2017 for Pien Island, Milillo et al 2019 for Thwaites). In my opinion this methodology might result misleading in areas where tidal amplitudes are small and is in fact providing wrong results. The authors should also comment on the discrepancies between the aforementioned studies.

We are unsure where this comment originates from. We state clearly in the manuscript that we could not map the grounding line in the ASE area, and hence we have not made any claims about grounding line retreat.

In line 126, we clearly articulate that we could not map the grounding zone in these areas:

"In the high sloping, low tidal range (0.8 m - 1 m) Amundsen Sea sector and the Amery Ice Shelf, we could not map a continuous grounding line."

The only place where the reviewer could have misinterpreted this is in line 245:

"In areas where the grounding line has significantly retreated (e.g. the Amundsen Sea sector), the coverage was too sparse to detect any change."

Which to avoid any further confusion, we have changed to:

"In areas where the grounding line has significantly retreated (e.g. the Amundsen Sea sector), we did not obtain sufficient coverage to map the grounding."

3) The authors compare their Cryosat2 results with DInSAR Grounding line measurements, However DInSAR data have not been acquired at the same time of the Cryosatdata. This important detail might result in a further misinterpretation of the results.

The area that we compared our results to, is known to be a stable area with no observed grounding line migration. Therefore, we are confident that comparing the results one year apart will lead to a negligible difference in grounding line location.

4) The authors use a simple elastic beam model to investigate the relationship between ice thickness and grounding zone width. The elastic model assume a fixed grounding line position whereas It has been proven in recent literature (Milillo et al 2017, Milillo et al 2019) that a simple elastic model does not explain tidally induced grounding line migrations commonly observed in nature.

We agree that a simple elastic model does not explain tidally induced grounding line migrations commonly observed in nature. It has also been proven in the literature that the simple elastic model does not capture the ice rheology, the motion of the ice sheet, grounding line geometry, or effects of tidal range. However, as we are comparing measurements of the grounding zone width over a large portion of the grounding zone of Antarctica, it was not feasible within the scope of this study to use a more complex model, as we have highlighted in this manuscript. We have now included tidally induced grounding migrations as another limitation of the model (line 243).

For these reasons I believe this study is still immature to be published in the proposed Journal.

We are disappointed in this review, in particular, comment 2, as this clearly shows the reviewer has not thoroughly read the manuscript. The other 3 criticisms are either beyond the scope of the study or only require minor changes which we have addressed in the relevant sections (as stated above).

REVIEWER 2

This paper uses Cryosat-2 data to map Antarctic grounding lines and tries to obtain additional information about the structure of the grounding zone. A large part of the paper describes the previous work, mapping methodology and results. This in itself is not novel (in fact it is well described already in Dawson & Bamber, 2017, GRL) and while the results are extended, and reasonable agreement is shown with previous studies, the mapping does not seem to be an improvement over previous maps.

While this method is not shown to be an improvement over previous studies, it can provide additional coverage that can contribute to the overall spatio-temporal mapping of the grounding zone. To support this conclusion, we have added another section titled (5. Coverage comparison with other methods). This section describes how the coverage of the CryoSat-2 data relates to other products. We show that there are several sections along the Filchner-Ronne Ice shelf that have previously only been mapped using break-in-slope methods. The previous grounding point F measurements that coincide with the new CryoSat-2 show no significant deviations. And while this does not show any spatial change in position, the results still confirm the location and stability of the mapped grounding zones.

The conclusion that ‘this method has the potential to monitor grounding line retreat and change in its structure’, while highly valuable if true, is not supported by the results. There is no demonstration of the ability to monitor change in grounding line position or grounding zone structure over the Cryosat-2 period, nor is it clear if the confidence in these results is high enough to establish change over longer periods by comparison

We agree that our results do not directly show the potential to monitor grounding line retreat, and therefore, we have removed this statement.

The title suggests the manuscript provides a method to obtain information on other grounding zone characteristics (besides position which is reasonably well known), but there are no substantial conclusions in this area. Is there any statistical significance between deviation from the grounding line width - thickness relationship and the other variables that influence ice response to tides in the grounding zone, such as plan-view curvature (i.e. concave - convex) or strain rate? These ’grounding zone characteristics’ could be obtained from the results themselves, or from auxiliary datasets and could lead to interesting findings. The observation of a correlation between grounding zone width

and ice thickness in-line with elastic beam theory has been shown before. In fact it is already discussed in a very similar way in Bindschadler et al., 2011.

Unfortunately, the data was too noisy for any statistically significant results to derive any firm conclusions. As a result, we have now removed lines 201-227 discussing the grounding zone structure, as we cannot reliably discuss any inferences about grounding zone characteristics. We have also altered the title of the manuscript to 'Measuring the location and width of the Antarctic grounding zone using CryoSat-2' as this changes the focus to mapping the grounding zone. However, the analysis using the elastic beam theory still provides valuable results as we have now calculated an effective Young's modulus of ice, which agrees well with previous methods.

Whilst the presentation is clear and concise, at present I feel this manuscript does not meet the standard for originality or significance required for publication in The Cryosphere. The main conclusion appears to be that Cryosat-2 tidal grounding line mapping agrees to some extent with previous studies, but does not increase accuracy, coverage or ability to monitor change. If the manuscript could be adapted to include any substantial new conclusions about grounding zone characteristics, structure or temporal or spatial change in position then it could still be a valuable contribution to the journal.

We thank the reviewer for their detailed comments and discussing weaknesses in the manuscript. We have now made significant alterations to the manuscript in response to these comments. We have now included a new section (5. Coverage comparison with other methods) detailing the additional coverage provided by this new dataset. This new section discusses the grounding line coverage provided by this method and other datasets, and while the mapped grounding zone mostly overlaps with previous methods, it still provides additional coverage, both spatiality and temporally.

As mentioned in previous responses, we could not perform any further analysis of the grounding zone structure. And in response to the reviewer's comments, we have removed the discussion on grounding zone structure beyond the simple elastic model as it did not provide any significant conclusions. The revised manuscript now highlights the valuable results of this research, while removing any inconclusive discussion present in the earlier version.

Specific comments:

L18: 'the freely'

corrected

L33: you suggest that 'DInSAR and ICESat do not have sufficient spatial or temporal coverage to monitor change across the entire grounding zone', but the method presented here also only maps 41% of the grounding zone. It is not clear what point is trying to be made and it is not clear that Cryosat-2 provides any improvement over these techniques.

CryoSat-2 data will not necessarily offer any improvements over DInSAR or laser altimetry techniques. However, despite only mapping 31% of the grounding zone, we do map point F for some sections of the grounding zone that have not been mapped in previous research (as this has been added to Section 5). See above for further discussions on this.

L39: How can you 'characterise' a stress gradient using tidal flexure information?

We agree this is ambiguous so have altered the statement to 'determine thickness and rheology across the grounding zone'

L50: This is not correct. Bindschadler et al., 2011 conducted a very similar analysis to yours for the entire continent.

We have altered to say 'mostly', Bindschadler et al., 2011 did investigate the grounding zone width over the entire continent. However, ours is the first study to compare grounding zone width calculated with tidal flexure information over a large percentage of the grounding zone.

L84: 'closely follows' the technique in Dawson & Bamber, 2017 or is the same? If there are minor differences it would help to say what these are, or if there are no differences, say so.

We have now clearly outlined in the revised manuscript where the methodology differs. In line 94, we state that we used an additional linear surface elevation rate, and in line 103 we explain that we used the moving window approach as we used 7.5 years of data instead of 3 years (as in the previous study).

L116: What is the justification for the 10km along track smoothing? Does this modify the positions significantly? What is meant by 'along track' in this context?

We have now changed along-track to along-line. The 10km smoothing does not modify the position of the grounding zone significantly and removes noise related to incorrectly mapping points F or H. This is now mentioned in line 133.

L138: It seems fairly arbitrary to say you would 'lose the resolution needed to map the grounding zone accurately'. What does 'accurately' mean here? How accurately is the grounding zone being mapped with the 2 km cells?

By 'accurately', we meant to be able to map with sufficient precision so that it is comparable to other methods and detect any changes in the grounding line position. We have now changed the wording (line 155).

This is effectively an arbitrary choice; however, we needed the data to be of comparable precision to previous methods. As we demonstrate in section 4.2, the CryoSat-2 grounding lines can be mapped with a standard deviation of 1.5 km compared to previous methods using a 2 km cell. This is similar to comparing different methods; for example, the DInSAR grounding line differs from the ICESat-1 grounding line by a standard deviation of 1.1 km. Therefore, using a larger cell size would lower the precision of the grounding zone map, and the results would not be comparable to other methods.

L149: A standard deviation of 1.7 km does not seem low (in comparison to your whole of Antarctica data). Tab1: I assume 'M' means MEaSUREs and 'E' means ESA CCI. Please specify in the caption.

You are correct, this has now been added

L172 / Fig 3: If there is no usable data from cross section C, just leave it out.

Agree

L179: Isn't the 10 km upper limit is self-imposed in the method? If you find grounding zones the full width then perhaps you need to expand the search region?

We have removed this sentence to avoid any confusion and added a sentence (line 129) clarifying that all mapped regions were below the 10 km limit.

Fig 5: Bedmap-2

Amended

L185: 'Poisson's ratio is generally denoted as 'nu' not 'mu'.

Agree and amended

L189: Rutford not Rutherford.

Agree and amended

L199: An attempt should be made to quantify these factors.

As mentioned previously the data is too scattered to attempt to quantify these factors.

L201-209: This is a valuable analysis. Can this be done for the whole dataset?

The data is too scattered to apply to the whole dataset and as a response to your earlier comments, we have removed this from the manuscript.

L219-222: How does this translate to variation in effective Young's Modulus? Is this factor actually related to change in ice properties or just to change in ability to monitor grounding zone width due to higher amplitude tides? Is there a difference between areas of semi-diurnal and diurnal tides?

We could not observe a difference between semi-diurnal and diurnal tides. As mentioned previously we have removed this section as without other statistically significant results the conclusion that this result can be believed is very weak.

L244: Cryosat & DInSAR

This section has been removed

L246: If this is the case it needs to be shown in the paper

This section has been removed

REVIEWER 3

The paper present results of a newly developed tool to map the grounding zone of Antarctic ice shelves from CryoSat-2 POCA and Swath data. The method was partly introduced by the authors in 2018 using a case study and was refined and updated and applied to whole Antarctica for the present study. In total 41% of the Antarctic grounding zone and its width could be mapped in an automatic way. The authors present in a clear and understandable way the method and compare the findings against independent grounding line data sets which were mapped using DInSar methodes. The standard deviation to those datasets is around 1km with regional differences. Additional the authors compare their results directly with cross section of DInsar interferograms from Sentinel 1 and can clearly show how well both methods match but also explain differences and shortcomings of their method.

In the last section they apply an elastic beam model to find a relation between ice thickness and grounding zone width with similar findings as Bindschadler (2011). The paper is well written, figures are clear and of high quality. The scientific outcome is of interest to the community, at least to my opinion, as it provides another independent data set of the grounding line and grounding zone width which is derived from Altimetry alone. I would like to thank the authors for this excellent work as the pre-processing already incorporates a full retracking of CryoSat-2 SARin data, the estimation of the POCA and a full interferometric swath processing. This dataset is then explored in a new way to derive grounding line and grounding zone width.

I do have some minor comments and questions.

1. Can you please argue why you selected a 3-year moving window to estimate 6- yearly measurements per grid cell which were then averaged instead of using the full time series or 5-year moving windows. I could imagine that with more data points per grid cell more tidal states are covered which might allow you better results in areas with low tidal signals or sparse coverage. I can

understand the argument with GL retreat however you mentioned that your approach was not able to detect a retreat in the Amundsen sector.

We have tested the full time series and the 5-year moving window per grid cell, and neither improved our results. As we mention in line 103, we used a 3-year moving window to account for any non-linear elevation change over the time period. And even though we were not able to obtain results over the grounding zones where this has occurred e.g. the Amundsen sector, this is still a good method to account for any variation like this, that may occur in areas where we have better coverage.

2. Please explain in more detail which criteria you used for the selection of SWATH and POCA data. I don't see any coverage of SWATH across the shelf ice, which makes sense as the SWATH shouldn't give useful information in flat terrain. However, Gourmelen et. al. showed some good results across Dotson. Is it possible to use Swath in the vicinity of Dotson as well in your study?

We used both POCA and swath data throughout the study where available in accordance to the processing parameters given in lines 74-75. There is also coverage of swath data over the ice shelves, as shown in Figure 1, where the ice shelves show a combination of POCA and swath data being used. The swath data improves coverage over the ice shelves particularly where there are crevassed regions. The majority of the data used is POCA where parts of the ice shelves are flat. However, we agree that we have not added sufficient detail regarding the use of POCA and swath data, particularly over the ice shelves and this has been added to line 84.

3. Please include in your validation against other grounding line data sets the ASAID dataset (Bindschadler, 2011) ASAID provides also the F and H lines and it would be a valuable information how much they differ and if you can see if and where H and F shows better agreement. Maybe you find some systematic difference.

We have not used the ASAID dataset for comparison as we wanted to compare methods that measured points F and H from tidal flexure information not the break-in-slope methods. However, this is a valuable dataset and we have now included it in section 5, discussing the location of the grounding lines from various methods.

4. Hogg et. al. (2017) mapped the grounding line from CryoSat-2 data as well. They used a different technique (break in slope) using only POCA data. Can you please show the differences to your data set and as reference to the ASAID one. It would be really interesting to see how much the additional use of Swath data and your new approach differs. Maybe in future one can find a combined approach to overcome shortcomings e.g. your approach has difficulties in areas of low tidal signal.

The Hogg 2017 grounding line measures the break-in-slope and as our method measures the limit of tidal flexure, they are effective measuring different things, thus combing the two would be difficult. Keeping them as separate but complementary products would be advisable.

5. Did you use a reference elevation model (REMA or global Tandem-X) to subtract topographic phase from your interferograms prior forming the DInSar interferogram? This might help to get rid of phase wrapping and to get a clearer picture in areas where you were not able to unwrap the DInSar phase (cross section C in Fig. 3, 4).

We used REMA in our processing, this information has been added to the manuscript (see line 179).

5. Your are following the method of Bindschadler et. al. 2011 to estimate a relation between width and ice thickness. Can you please apply the fit to different regiones to see if you can reduce the spread in cases of low measurement error. Can you please derive your best fit using another Young modulus to show the influence of E. e.g. Rack et. al. 2017 used 1.5 Gpa to analyse the tidal flexure in the grounding zone and where able to account for horizontal motion in DInSar derived grounding

line position. Whereas Wild et. al. 2019 found 1.0 +/- 0.56 GPa as best fit to tiltmeter measurements and a numerical model.

We did not derive our results with any Young's modulus as this is a parameter which is calculated within the fit, and can be derived, if we use assumptions for seawater density and the Poisson ratio of ice. We have now modified this section to explain this more explicitly. We also derived a Young's modulus from this work with E=1.4 ± 0.9 GPa, which agrees well with previous studies. As mentioned in the response to reviewer 2, the data was too noisy to make any further comparisons, for example, we did not see statistically significant results between different regions.

Figures:

Please note which grounding line you used in the figures 1,2, A1 and A2 Fig 1 and A2: Please change the colour scale. Red-Green blind people can't see anything.

We have added the grounding line used in the Figure caption. We found it extremely difficult to have a suitable colour scale in Figures 1 and A2 as we include intensities as well as three different scales. Instead we have added a new Figure (A3) which is a replication of A2 but with a colour-blind safe scale without intensity values.

Fig 3: Why did you select cross section C in Figure 3 as validation against DInSar? It would be also worth to show a second DInSar pair from a different tidal state, to illustrate how much the width of the fringe belt can vary. Maybe you can include the F and H line of the ASAID data set as well.

We have removed cross section C. We used this DInSAR data as the difference in tides between the two scenes is 1.1m and this is similar to the average displacement due to tides over the Ronne Ice Shelf. As the CryoSat-2 method effectively measures the average of point F and H as it samples the grounding zone over a long period of time, therefore using this image is a fair comparison. We have added a sentence in line 186 to discuss this point. We agree that investigating point F and H in relation to different tidal amplitudes would be an interesting study, however this would not provide any further validation for out CryoSat-2 data.

Fig 6: Please double check the number and citation and the position of the blue line. Bindschadler (2011) derived 22.2 +/- 6.2 referring to values estimated by Vaughan (1995). Typo: Please double check the numbers given for X in line 191 and 204 and Fig 6.

Checked and altered

REVIEWER 4

In their TCD manuscript "Antarctic grounding zone characteristics from CryoSat-2" Dawson and Bamber employed CryoSat-2 data to map 41% of the main floating ice shelves and outlet glaciers of Antarctica. The used method closely follows the one described by Dawson and Bamber (2017) but uses 7.5 years of Cryosat-2 data and is applied to the whole of Antarctica. In contrast to their previous study the authorsestimate the width of the grounding zone by fitting an error function to their CryoSat2 estimate and compare their results with grounding zone estimates from Sentinel-1DInSAR.

General remark:

Overall I find the manuscript is well written and interesting to read. I like the way how CryoSat-2 data is employed here as the proposed method is much more sophisticated than previous break-in-slope assumptions of the grounding line. However, considering the limitations of the method it is difficult to judge where the results are trustworthy and where not. I therefore suggest to include a reliability map which utilizes the combined effect of tidal range and data coverage. This should result

in reasonable results at high latitudes – i.e. regions which are only sparsely covered by grounding line estimates from DInSAR due to orbital constrains.

Although we have not included a reliability map made from information about the data coverage and tidal range, we have now added a map of the standard deviation of T_d (calculated from the yearly measurements). This map can act as a guide to the reliability of the data. We have included a description in lines 113-115 and discussed the results in lines 169-170. We find the standard deviation is lowest in the high tidal range areas and high latitude areas while it increases to the low tidal range and low latitude areas. These results closely match what we observe in comparison with DInSAR and ICESat-1 measurements.

To strengthen the study I would also put more emphasizes on the latter point which should be mentioned in the abstract and conclusion.

We have now included this point in the abstract and conclusion and has been discussed in the new section (5. Coverage comparison with other methods)

Further, I encountered several flawless mistakes which need to be corrected and are partly listed in the following. Please be consistent with the terms “grounding line” and “grounding zone”.

Specific comments:

Line 18: typo, “thefreely”.

Amended

Line 23: include “in” before grounding line location.

Amended

Line 26: remove “of”.

Amended

Line 27: I presume you mean satellite remote sensing here?

Yes and amended

Line 29-31: maybe you could already state here that the term “grounding line” refers to point F throughout the manuscript.

Agree and amended

Line 34: what is meant by “entire grounding zone”? Not clear.

Changed to ‘across all the Antarctic grounding zone’

Line 111-112: are you really referring to the grounding line (i.e point F) here? Please clarify.

Yes, and based on your previous comment we have now explicitly mentioned the grounding line refers to point F.

Line 114: I am not sure what is meant by grounding line width? Are you referring to the grounding zone width here?

Agree and amended

Line 120: 41% relative to what? Please state which ice shelves and outlet glaciers are defined as “main”, otherwise this number is worthless. Maybe it is more appropriate to state that you were

able to map 31% of the grounding zone surrounding Antarctica (at least according to your Table 1). This also applies for the abstract.

Agree and amended

Line 121-122: I think this is a very important point, as these are the critical areas for DInSAR estimates due to orbital constrains. Here only few coherent left looking acquisitions are available from TerraSAR-X and RADARSAT drawing a rather incomplete picture of the grounding zone. Further, break-in-slope estimates are far off due to gentle slopes in the area. It would certainly strengthen the manuscript if more emphasizes would be on this point.

We have added a new section that highlights this point titled '5. Coverage comparison with other methods'. In this section, we describe in detail the grounding line coverage provided by this method compared to other datasets, and we show there are some areas in the high latitude areas that have not been mapped using DInSAR.

Line 131: maybe you could also cite Gourmelen et al., 2017 here as their study is also based on CryoSat-2.

Yes

Line 142: I am wondering why the results are not compared to the ones from Bindschadler et al., 2011?

We did not want to compare these results directly with Bindschadler et al., 2011 as these results are from break-in-slope methods. However, we have added a comparison with this dataset in section 5

Line 181: I am not sure what you mean by grounding line width? Width of the grounding zone? If so, please change here and elsewhere.

Agree and amended

Line 201-209: this could potentially be shown in Figure 4.

We have now removed this section in response to reviewer 2.

Line 211: grounding zone?

We have now removed this section in response to reviewer 2.

Line 211: are you sure you are referring to ice thickness here?

We have now removed this section in response to reviewer 2.

Line 220: include "to" before "tides".

We have now removed this section in response to reviewer 2.

Line 224-226: true, therefore I find the section title "Grounding zone structure" a little bit misleading.

We agree and we have now changed the title to be 'Grounding zone width'

Figure 1: which grounding line is shown here? This needs to be cited in the caption as it is certainly not the one derived in this study.

Agree and amended

Figure 4: please state in the caption that you were not able to unwrap the fringe belt at the location of profile C.

We have now removed profile C from the figure.

Figure 5: “Grounding line width, W” has never be mentioned in the text. I am not really convinced about the information content of this Figure and would rather move it to the appendix. Instead I would include a reliability map into the main manuscript as mentioned in my general remark.

The map grounding zone width is discussed in section 6 and provides valuable information about the spatial distribution of the width of the grounding zone, and therefore should be left in the main text. However, in response to the earlier comment, we have included a map that gives a measure of the reliability of the data (this has been included in the appendix).

Measuring the location and width of the Antarctic grounding zone characteristics from using CryoSat-2

Geoffrey J. Dawson[1] and Jonathan L. Bamber[1]

[1]Bristol Glaciology Centre, School of Geographical Sciences, University of Bristol, Bristol, UK

Correspondence: Geoffrey J. Dawson (geoffrey.dawson@bristol.ac.uk)

Abstract. We present the results of mapping the limit of tidal flexure (point F) and hydrostatic equilibrium (point H) of the grounding zone of Antarctic ice shelves from CryoSat-2 standard and swath elevation data. Overall we were able to map 4131 % of the grounding zone of the larger Antarctic floating ice shelves and outlet glaciersin Antarctica. We obtain near-complete coverage of the Filchner-Ronne Ice Shelfand . Here we manage to map areas of Support Force Glacier and the Doake Ice Rumples, which have previously only been mapped using break-in-slope methods. While we obtained and partial coverage of the Ross Ice Shelf, Dronning Maud land Land and the Antarctic Peninsula , while and we could not map a continuous grounding zone for the Amery Ice Shelf and the Amundsen Sea Sector. Tidal amplitude and distance south (i.e. across track across-track spacing) are controlling factors in the quality of the coverage and performance of the approach. The location of the point F agrees well with previous observations that used differential satellite radar interferometry (DInSAR) and ICESat-1, with an average landward bias of 0.1 km and 0.6 km and standard deviation of 1.1 km and 1.5 km for DInSAR and ICESat measurements, respectively. We also compared the results directly with DInSAR interferograms from the Sentinel-1 satellites, acquired over the Evans Ice Stream and the Carlson Inlet (Ronne Ice Shelf) and found good agreement with the mapped points F and H. We also present the results of the spatial distribution of the grounding zone width (the distance between points F and H), and used a simple elastic beam modelto investigate the relationship between ice thickness and grounding zone width, along with ice thickness calculations, to calculate an effective Young's modulus of ice of $E = 1.4 \pm 0.9$ GPa.

1 Introduction

In Antarctica, the majority of the grounded ice sheet (74 %, *Bindschadler et al.* (2011)) abuts floating ice shelves or outlet glaciers. It is in this grounding zone where the ocean can directly influence the inland ice sheet. The grounding zone delineates the different stress regimes of grounded and freely floating ice. Grounded ice that was once supported by the bed is transitioning to thefreely the freely floating ice shelf, and is supported partially by internal stresses and by hydrostatic pressure. The precise point at which the ice sheet detaches from the bed (i.e. the grounding line) may vary on short time scales modulated by tidal motion and bedrock slope. Ice thickness, basal drag and side drag may also vary across the grounding zone, causing rapid changes in ice velocity. Understanding ice dynamics and structure across the grounding zone is important for mass budget calculations and makes it a critical boundary for ice sheet modelling. In areas of low bedrock slope, changes in ice thickness in the grounding zone can lead to large horizontal changes in grounding line location. For example, grounding line retreat in

the Amundsen Sea Sector (*Rignot et al.*, 2014; *Christie et al.*, 2016; *Scheuchl et al.*, 2016), caused by dynamic thinning of this part of the ice sheet (*Shepherd et al.*, 2002; *McMillan et al.*, 2014), has highlighted the need to monitor changes in grounding zone location as ~~one measure of~~ a measure of ice sheet stability.

It is not possible to ~~remotely~~ measure the actual location of the grounding line ~~, instead,~~ with satellite remote sensing. Instead, we can study ice shelf flexure or surface geometry (such as ~~break in slope~~break-in-slope) to infer its position. The inner limit of tide-induced ice sheet flexure (point F), is commonly used as a proxy for the grounding line (and from here on, we will refer this as the grounding line). Point F can be mapped using differential satellite radar interferometry (DInSAR) (*Gray et al.*, 2002; *Rignot*, 1998b), repeat track analysis of ICESat (Ice, Cloud, and land Elevation Satellite) laser altimetry (*Fricker and Padman*, 2006) and CryoSat-2 radar altimetry (*Dawson and Bamber*, 2017). We can also identify the point past which the ice shelf is in hydrostatic equilibrium (point H), providing a measure of the width of the grounding zone, W, (i.e. the distance between points F and H, *Fricker and Padman* (2006)). However, currently DInSAR ~~or~~ and ICESat techniques do not have sufficient spatial or temporal coverage to monitor ~~change across the entire~~ changes across all the Antarctic grounding zone. Break-in-slope methods (*Bohlander and Scambos*, 2007; *Bindschadler et al.*, 2011; *Bamber and Bentley*, 1994; *Hogg et al.*, 2017) between the flat ice shelf and the grounded ice sheet ~~can also allow~~ also allows us to map the grounding line~~and monitor retreat~~, but in regions where there is not a clear ~~break in slope~~break-in-slope, this technique can be unreliable or ambiguous (*Bamber and Bentley*, 1994; *Fricker and Padman*, 2006; *Brunt et al.*, 2010; *Rignot et al.*, 2011; *Depoorter et al.*, 2013). It is over these regions where ice thickness does not increase rapidly across the grounding zone, that grounding line retreat is most likely and there is good spatial and temporal coverage using DInSAR techniques. Over regions where ice thickness increases rapidly inland, and the ice sheet is not thinning, DInSAR coverage is more variable, especially in the high latitude areas where there is limited coverage due to orbital constraints of the satellites. Using CryoSat-2 data in these areas could provide a more complete coverage of point F.

We can also use the tidal flexure of the ice sheet to investigate the structure of the grounding zone. This can help ~~us characterise stress gradients and ice rheology .~~ determine thickness and rheology across the grounding zone. Studies that have investigated the structure of the grounding zone through tidal flexure have, to date, mostly focused on individual ice streams. *Holdsworth* (1977) first used an elastic beam model as an analogue for the grounding zone. This enabled studies that used tilt-meters (*Stephenson*, 1984) and kinematic GPS methods (*Vaughan*, 1995) to measure the tidally ~~induces~~ induced deformation across the grounding zone and determine the elastic (Young's modulus) properties of the ice. More recently, DInSAR was used remotely to measure the magnitude of the tidally ~~induces~~ induced deformation across the grounding zone (*Rabus and Lang*, 2002; *Sykes et al.*, 2002), and was combined with numerical elastic models (*Schmeltz et al.*, 2002; *Marsh et al.*, 2014) to estimate ice thickness distributions and ice properties across the grounding zone. These studies have shown that the measured Young's modulus differs substantially from laboratory measurements. Fracturing in the ice can reduce its effective thickness (*Hulbe et al.*, 2016; *Rosier et al.*, 2017), and the elastic modulus can vary through changes in temperature and ice fabric. The ice also does not behave purely elastically over the timescales of tidal motion, and this can be investigated by treating it as a viscoelastic material (*Wild et al.*, 2018).

Studies that have investigated the structure of the grounding zone through tidal flexure have, to date, focused on individual ice streams. The method presented here uses CryoSat-2 radar altimetry to provide a new tool that allows us to map a large points F and H of a significant fraction of the grounding zone, while also investigating its structure. In this paper, we first present the results of using 7.5 years of CryoSat-2 data to map the Antarctic grounding zone. The results are then validated against previous DInSAR and ICESat measurements. Finally, the grounding line width, ~~W~~ W (the distance between point F and H) is then used to investigate the physical structure , in combination with independent ice thickness measurements and the simple elastic beam model of the grounding zone to investigate its structure.

2 CryoSat-2 Data

CryoSat-2, launched in 2010, uses a synthetic aperture radar interferometric (SARIn) mode near the margins of the ice sheet. This new mode mostly overcomes issues of off-ranging and "loss-of-lock" near breaks in slope breaks-in-slope, which have limited the coverage of conventional satellite radar altimetry over sloping terrain (*Bamber et al.*, 2009). The SARIn mode combines "delay-Doppler" processing to improve along-track resolution (*Raney*, 1998), with dual antennas to provide the location of the return echo in the cross-track direction (*Jensen*, 1999). This enables the acquisition of elevation measurements based on the first return (point of closest approach or POCA) and "swath processed" heights derived from the time-delayed waveform beyond the first return (*Gray et al.*, 2013). In this study, we used CryoSat-2 POCA and swath elevation data , to measure elevation change due to tidal flexure of the floating ice shelf. These data were derived from the CryoSat-2 SARIn baseline C level 1b product, with revised star tracker measurements provided by the European Space Agency (ESA). We processed POCA data using the scheme described in *Helm et al.* (2014) which employs a threshold re-tracker , as this is less sensitive to any changes in the extinction coefficient of the snow and minimises any potential biases in elevation data. We used a processing scheme that closely follows *Gray et al.* (2013) to process the swath data, and used minimum coherence and power thresholds of 0.8 and -160 db, respectively.

The coverage of POCA and swath data is shown in Figure 1 and Figure A1 (with a simpler plot provided in A2). POCA data provides consistent sampling over flat terrain, such as ice shelves with higher data density at high latitudes due to the narrower track spacing of the satellite. However, as they are based on the first return of the waveform, over sloping terrain, they only provide elevation measurements upslope of satellite nadir. This reduces coverage, particularly near a break in slopebreak-in-slope, such in the vicinity of the grounding line. Swath data provides elevation estimates downslope of POCA, and to obtain the best coverage of the grounding zone, we need to use a combination of POCA and swath data. While swath data tends to be noisier (*Gray et al.*, 2017), they have an order of magnitude higher spatial sampling than POCA data. We obtain the highest sampling of swath data near breaks in slopebreaks-in-slope, and over moderately sloping terrain. Over the ice shelves, swath data provides improved coverage in crevassed regions, however over the flat regions, the majority of data used is POCA. In high sloping regions areas with complex topography, we generally lose coverage, for example, the Transantarctic Mountains and parts of the Antarctic Peninsula. In these regions, steep slopes can cause the satellite to lose "lock" wherein the return echo of the radar wave is not captured within the range window. Also, in areas of complex topography, there may be more than one

point where the radar wave reflects off the ground for a given range, leading to a loss of coherence and an ambiguous location for the located echo in the cross-track direction.

3 Methods

Our approach used CryoSat-2 surface elevation measurements to determine the limit of tidal flexure of the ice (F) and the limit of hydrostatic equilibrium (H), and closely followed the technique described in *Dawson and Bamber* (2017). The key feature of this approach is to use the pseudo-crossover method of *Wouters et al.* (2015), to simultaneously solve for topography, a dimensionless tidal amplitude (T_d) and, additionally in this study, a linear surface elevation rate ($\dot{h}$) using equation (1).

$$h(x,y,p) = a_0 + a_1.x + a_2.y + T_d.p + \dot{h}t \quad (1)$$

Where h is the elevation, t is time, a_0 is the mean elevation, a_1 and a_2 are the slopes of the topography in the x and y direction respectively. We used a model tidal amplitude, p, (the CAT2008a tide model, which is an update to the model described by *Padman et al.* (2002)) calculated at a constant distance of 10 km from the nominal grounding line in *Depoorter et al.* (2013) to scale T_d. Thus, T_d gives a measure of the tidal contribution to the elevation, and $\dot{h}$ ~~measures~~ MEaSUREs elevation change not associated with tidal motion e.g. from ice sheet thinning or changes in firn compactions rate of the floating ice. Also as we are calculating T_d over position over a 3 year window, this method cannot capture any dynamic changes that may have occurred over this period.

We calculated T_d (Figure 2) and $\dot{h}$ (Figure ~~A2~~A3) within a 2×2 km grid cell using CryoSat-2 data between 2010 and 2017. ~~We~~ As we are using 7.5 years of data compared to 3 years as in our previous study, we used a 3-year moving window, weighted by a tri-cube weight function, resulting in 6 yearly measurements for each grid cell between 2011 and 2017. ~~By using~~ Using a 3-year moving window, we ensured that there were at least 4 different satellite passes per grid cell while allowing for any dynamic changes in elevation of the ice sheet that may have occurred. An alternative method would be to calculate temporal changes in T_d and $\dot{h}$ over the entire time series. This would require including additional parameters, ~~however,~~ which may risk over-fitting the data. We then calculated the mean of T_d, to obtain a single value over the observation period ~~. We~~ and only used data where $-0.5 < T_d < 1.5$ and $|T_d - \tilde{T}_d| < 0.5$ where $\tilde{T}_d$ is the median values of the yearly measurements per cell. This removed any poor fits to equation ~~1~~(1), which likely come from erroneous elevation data. This method could potentially monitor grounding line retreat, for example, in the Amundsen Sea Sector (*Rignot et al.*, 2014; *Christie et al.*, 2016; *Scheuchl et al.*, 2016)~~. However, as these areas have a small range of tidal amplitude and poor data coverage~~ , however we could not map a continuous grounding line in these areas (see Section 4.1)~~, we could not detect a significant change during the observation period (2010-2017).~~ . To display the reliability of this method, we have included a map of the standard deviation of T_d used in calculating point F and H (Figure A4). The lowest standard deviations are found in the high latitude, high tidal range areas of the Ross Ice Shelf and the Filchner-Ronne Ice Shelf, while over the lower latitude areas where coverage is sparser the standard deviation is high between yearly measurements.

When ice is in hydrostatic equilibrium, the real tidal amplitudes match the closest model tidal amplitudes, and we find $T_d = 1.0 \pm 0.2$. Over grounded ice, we find $T_d = 0.0 \pm 0.2$, as there is no correlation between elevation and model tidal amplitudes.

Previously we mapped ~~the~~ point F by considering ice to be influenced by the vertical motion of the tides above a certain threshold. This introduced a seaward bias, as we did not resolve amplitudes below the threshold value. In this study, we fitted an error function perpendicular to the grounding zone to determine ~~*F and H*~~F and H, and removed any potential bias. This process was performed iteratively: We first mapped the centre line of the grounding zone (i.e. $T_d = 0.5$ contour) with a 1000 m spacing. We then sampled T_d perpendicular to the initial guess of the centre line of the grounding zone, and fitted an error function to find a new location for $T_d = 0.5$ as well as points F ($T_d = 0.1$) and H ($T_d = 0.9$). The centre line of the grounding zone was then re-sampled to 1000 m spacing, and the process repeated. The process was repeated at least three times or until the grounding line location did not change significantly by visual inspection. To make the fitting method more robust, we fixed the maximum and minimum value to 1 and 0, respectively, and weighted the fitting process around $T_d = 0.5$, using a tri-cube weight function. We only included data points where the grounding ~~line~~ zone width was calculated between 100 m and 10000 m, and where there was continuous coverage of T_d across the grounding zone. ~~We~~ Before imposing the 10000 m upper limit grounding line width, we verified that no mapped regions were wider than this, and we only removed poorly fitting data. We then split the grounding line when there was a break greater than 4 km, and removed any segments of mapped grounding line shorter than 20 km. Finally, we applied a 10 km ~~along-track~~ along-line smoothing using the Polynomial Approximation with Exponential Kernel (PAEK) smoothing algorithm, this removed along-line noise related to incorrectly mapping points F or H, but did not significantly alter their locations.

4 Grounding zone mapping

4.1 Coverage

We were able to map the grounding zone (points F and H) for ~~41~~31 % of the ~~main~~ Antarctic floating ice shelves ~~or~~ and outlet glaciers. The percentage mapped for several key regions are shown in Table 1. In the high latitude areas of the Ross Ice Shelf and the Filchner-Ronne Ice Shelf, we obtained ~~near complete~~ near-complete coverage. In these regions, the track spacing of CryoSat-2 is as low as 0.5 km resulting in a high spatial sampling of the grounding zone, and we only lost coverage in high sloping regions with complex topography, for example, the Transantarctic Mountains.

At lower latitudes, further north, the coverage is variable. The spatial sampling is lower as the track spacing of the satellite varies from 2 km to 3 km. In the high sloping, low tidal range (0.8 m - 1 m) Amundsen Sea ~~sector~~ Sector and the Amery Ice Shelf, we could not map a continuous grounding line. There were very few POCA data near the grounding zone, and the swath data were too noisy to resolve the tidal signal. Also, over fast-flowing ice shelves such as Pine Island and Thwaites glacier, any surface features such as ridges will move along the direction of flow. As the surface is not sampled at the same time, this will result in a spread of elevation measurements over these features, introducing noise. Using a Lagrangian framework to correct for the movement of the ice shelves, is an effective way of removing this source of noise ~~(*Moholdt et al.*, 2014)~~ (*Moholdt et al.*, 2014; *Gourmelen et al.*, 2017). However, a Lagrangian framework cannot be used in this study, as it is only valid ~~on~~ for floating ice shelves and not over grounded ice or the grounding zone.

The coastline of Dronning Maud Land is also at relatively low latitudes~~, however~~. However, the tidal range is higher (1 m - 2 m) and we were able to resolve the tidal signal using primarily swath data. ~~Here, we~~ We obtained 41 % coverage of the grounding zone for Dronning Maud Land. In the lower latitude areas of the Antarctic Peninsula, the track spacing of the satellite ranges from 3 km to 4 km. The spatial sampling of both POCA and swath data is lower, and we were able to map 11 % of the grounding zone. To improve the coverage in low latitude areas we could have increased the cell size from 2 km, however, we would then ~~lose the spatial resolution needed to map the grounding zone accurately~~not have sufficient precision to be able to compare to other methods and detect if the grounding line position has changed.

4.2 Validation with DInSAR and ICESat observations

We first compared point F mapped using CryoSat-2 to ~~the~~ previous mapping methods that used DInSAR observations (*Rignot et al.*, 2016; *ESA Antarctic Ice Sheets CCI*, 2017) and ICESat (*Brunt et al.*, 2010) repeat-track analysis. The absolute distance (or bias) and the standard deviation between the CryoSat-2 grounding line (defined as point F here) and the DInSAR/ICESat grounding lines for several regions are shown in Table 1. Across the whole of Antarctica, the absolute distance between the DInSAR and ICESat ~~groundings~~ grounding lines and the CryoSat-2 grounding line is -0.1 km (a negative value represents a landward bias) for both datasets, showing that there is a negligible landward bias between the CryoSat-2 method and others, which does not change significantly with region. The standard deviation is 1.1 km and 1.5 km between the DInSAR and ICESat ~~groundings~~ grounding lines and the CryoSat-2 grounding line, respectively, however, this varies with region. In the high latitude areas of the Ross and Filchner-Ronne Ice Shelves, the standard deviation is low (~~1.7~~1.0 km between the CryoSat-2 and DInSAR grounding lines), and the grounding line matches well. While in the lower latitude areas with large tidal range (Dronning Maud land and ~~Amery Ice Shelf~~Antarctic Peninsula), there is a standard deviation of ~~2.0~~1.3 km between the CryoSat-2 and DInSAR grounding lines. This increase in standard deviation is due to reduced data density at lower latitudes, and also the smaller tidal range, which results in a noisier calculation of T_d and a larger deviation from previous observations. This larger variability in mapping is also shown in the standard deviation of T_d (Figure A4), where the largest standard deviations are found over the Dronning Maud land and Antarctic Peninsula. In comparison, the grounding line mapped using *Rignot et al.* (2016) has a bias of -0.3 km with a standard deviation of 0.9 km when ~~it is~~ compared to the *ESA Antarctic Ice Sheets CCI* (2017) grounding line and a bias of -0.4 km with a standard deviation of 1.1 km when compared to the ICESat grounding line.

We also compared our results directly with DInSAR interferograms from the ~~Sentinel-1~~ deviations-1 satellites, acquired over the Evans Ice Stream and the Carlson Inlet (Ronne Ice Shelf). We used single look complex (SLC) SAR images acquired by the Sentinel-1 satellites in the interferograms wide swath mode. The SAR operates in the C-band at 5.405 GHz, and in the wide swath mode, ~~lead~~ leads to a 5x20 m resolution in ground range and azimuth. Each satellite has a repeat cycle of 12 days, and by using both Sentinel-1A and 1B, we were able to form the double-differenced interferograms from 3 scenes spanning between 21st July and 3rd August ~~2018, and~~ 2018. The data were processed using GMTSAR, with the effects of topographic phase being removed using the Reference Elevation model of Antarctica (REMA) (*Howat et al.*, 2019). By calculating the difference between two interferograms, we removed any signal that is common ~~among~~ to both interferograms, (e.g. constant ice flow) and only measured changes in ice flow and deformation of the ice sheet. This region of the Filchner-Ronne Ice Shelf is a relatively

Table 1. The percentage of grounding line mapped along with the bias (a negative value represents a landward bias) and standard deviation between the CryoSat-2 mapped grounding line (Point F) and the DInSAR ((M)EaSUREs, and (E)SA CCI) and ICESat mapped ~~groundings~~ grounding lines, for several regions across Antarctica (shown in Figure 1)

Area	% mapped	Bias (km)			Standard deviation (km)		
		DInSAR (M)	DInSAR(E)	ICESat	DInSAR (M)	DInSAR (E)	ICESat
Antarctica	32	- 0.1	-0.1	- 0.6	1.1	1.2	1.5
Filchner-Ronne Ice Shelf	90	-0.1	0.1	- 0.6	1.1	1.2	1.2
Ross Ice Shelf	43	-0.1	-0.1	- 0.6	0.9	1.0	1.5
Dronning Maud Land	41	0.1	0.3	-0.9	1.2	1.3	1.9
Antarctic Peninsula	11	-0.1	-0.1	–0.6	1.3	1.2	1.9

stable area, and over the time frame of measurement, any elevation change will likely be due to tidal deformation. This results in very little measured deformation over grounded ice and a series of interference fringes that corresponds to the change in height between the two interferograms due to tides. The landward and seaward limit of these fringes can be robustly interpreted as point F and H, respectively. We also chose scenes where the tidal deformation was an average of 0.8 m. CryoSat-2 gives an average of point F and H as it samples the grounding zone over a long time, and using a deformation close to the average, we reduced any potential difference in points F and H due to tidal amplitude.

The double difference interferogram is shown in Figure 3, and the inner and outer limit of interference fringes which correspond to the boundaries of the grounding zone agree well with the mapped points F and H from CryoSat-2. Each fringe corresponds to approximately 2.8 cm change in height, and by unwrapping the interferogram using the snaphu method (*Chen and Zebker*, 2001), we were also able to compare the difference in height caused by tidal deformation. ~~Three~~ Two cross-sections over the Evans Ice Stream and the Carlson Inlet are shown in Figure 4, and by normalising the deformation, we could compare the results directly for two cross-sections (the third cross-section did not have any usable SAR data). In both cross-sections T_d approximately matches the deformation measured by DInSAR and points F and H match well. However, T_d does not match the exact shape of the deformation. In the DInSAR data, we observe a sharp transition between fully grounded and partially grounded ice and a smoother transition to fully floating ice. This detail is not captured by CryoSat-2 as it does not have the precision to detect these small changes in elevation to resolve the tidal deformation fully.

5 ~~Grounding zone structure~~Coverage comparison with other methods

In this paper we focus on the Filchner-Ronne Ice Shelf and the coastline of Dronning Muad Land. Over these regions and the Siple Coast region of Ross Ice Shelf, we obtained sufficient coverage of the grounding zone that allowed us to compare, and potentially add, to the existing grounding line map. The coverage over the Siple Coast region of Ross Ice Shelf was detailed in *Dawson and Bamber* (2017), highlighting that the grounding zone over the Echelmeyer Ice Stream was approximately 25 km inland from the previous grounding line estimate of ICESat and break-in-slope methods.

For the coastline of Dronning Maud Land, the MEaSUREs and the ESA CCI grounding line have near-complete coverage of the grounding zone (98%), and CryoSat-2 has mapped no new locations. Over areas where there is coverage, we observe no significant deviation from the previous products. The DInSAR mapped grounding lines were recorded between 1992 and 2014 and between 1995 and 2017 for the MEaSUREs and the ESA CCI grounding lines respectively. This indicates no observable change in the grounding line position between then and the current measurements of CryoSat-2.

Overall the MEaSUREs and the ESA CCI grounding lines provide 91% and 66% coverage of the grounding zone for the Filchner-Ronne Ice Shelf, with a combined coverage of 97%. Over the regions where the mapped CryoSat-2 grounding zone coincided with DInSAR measurements, again, we observed no significant deviations. However, there are some areas over Support Force Glacier and the grounding zone around the Doake Ice Rumples which have not been mapped using DInSAR shown in Figure 5. These regions have previously been mapped only using break-in-slope methods (e.g. the Antarctic Surface Accumulation and Ice Discharge (ASAID) project grounding line (*Bindschadler et al.*, 2011)), and we can see the Doake Ice Rumples where the grounding zone matches well. However, over Support Force Glacier, there are several places where point F is measured by CryoSat-2 differs from the break-in-slope of the ice sheet of more than 10 km. These are areas where there is no clear break-in-slope, and the grounding line has likely been incorrectly mapped.

6 Grounding zone width

The width of the grounding zone (~~X~~W), is shown in Figure ~~5~~ 6 for several regions across Antarctica ~~. X ranges between 0.5 km and 10 km and~~ and has a strong regional variation. The widest grounding zones were found over the Mercer (Ross Ice Shelf), Institute and Möller Ice Streams (Filchner Ice Shelf)~~. While~~ , while the narrowest regions were found over ice shelves of Dronning Maud Land. To a first approximation, this variation in grounding ~~line~~ zone width can be attributed to the ice thickness ~~in~~ of the grounding zone (see Figure 5). The thicker ice tends to be more inflexible, and consequently the internal stresses of the ice can support the ice further from point F. We can demonstrate this by modelling the grounding zone as a semi-infinite beam of constant thickness (*Holdsworth*, 1977). With this model, the vertical deflection of the beam (w) is described by

$$w(x) = A_0[e^{-\beta x}(\cos\beta x + \sin\beta x)] \tag{2}$$

where the beam is pinned at a hinge line at ~~x~~ x = 0 and it is displaced vertically by A_0. The spatial wavenumber, β, is given by

$$\beta^4 = 3\rho_w g \frac{1-\mu^2}{Eh^3}\frac{1-\nu^2}{Eh^3} \tag{3}$$

where h is the ice thickness, E the Young's modulus, ~~μ~~ ν the Poisson ratio, ~~ρ_w~~ $\rho_w = 1026$ kg m^{-3} the density of seawater and g the acceleration due to gravity. Given this relationship, the strongest dependence on spatial wavenumber is the thickness of the ice. *Bindschadler et al.* (2011) used this relationship, the elastic properties of ice (~~$\mu = 0.3$ and $E = 0.88$ GPa~~$\nu = 0.3$ and $E = 0.88 \pm 0.35 GPa$) and parameters from the ~~Rutherford ice stream~~ Rutford Ice Stream (*Vaughan*, 1995) to estimate the grounding line width, ~~$X = (22.2 \pm 6.2)h^{3/4}$~~$W = (22.2 \pm 6.2)h^{3/4}$. If we compare ~~$X$~~ W to ice shelf thickness measurements (*Chuter and Bamber*, 2015) at point H calculated from CryoSat-2 POCA elevation data using the assumption of hydrostatic

equilibrium, we find ~~$X = (26.4 \pm 6)h^{3/4}$~~ $W = (26.4 \pm 6)h^{3/4}$, which agrees well with the previous relationship (Figure ~~6).~~ 7). This also allows us to directly derive an effective Young's modulus of ice as $E = 1.4 \pm 0.9$ GPa, using $\nu = 0.3$.

There is considerable scatter between these results due to significant measurement ~~error~~ errors from both h and ~~X~~ W and because other factors ~~,~~ such as ice rheology ~~,~~ vary regionally. Ice shelf thickness measurements have shown to have a mean percentage error of 4.7% near the grounding zone of the Amery Ice ~~shelf~~ Shelf (compared to radio echo sounding measurements (*Chuter and Bamber*, 2015)). These errors could be larger in some areas, ~~due,~~ for example, due to uncertainties in firn compaction in areas of compressive flow (*Bamber and Bentley*, 1994) and ~~varitions~~ variations in damage mechanics along shear margins. These parameters may vary over areas where there are rapid changes in ice dynamics and bed topography ~~, such as the grounding zone,~~ potentially introducing larger errors. The grounding zone width is also dependent on ice rheology, the motion of the ice sheet, grounding line geometry~~and ,~~ tidal range and ~~all these factors will also contribute~~ grounding line migration, with these factors also contributing to the observed scatter.

~~The effect of grounding zone shape can be seen if we look at two cross-sections over the Evans Ice Steam (profiles B and C in Figures 3 and 4). Profile B is situated over a concave section of grounding zone, while profile C is over a straight section of grounding zone. The ice thickness at point H is 868 m and 717 m, and this corresponds to an estimated grounding zone width of 3550 m and 3075 m, using the simple model of the grounding zone, $X = (25.4 \pm 6.2)h^{3/4}$, for the concave and straight section, respectively. The model grounding zone width for the profile C is overestimated by approximately 10% (the measured width is 2984 m), while there is a larger discrepancy with the model grounding zone width for the concave section, which is underestimated by 18% (measured width 4220 m or 4560 m using DInSAR). This is because the concave shape allows internal stresses to provide support over a longer distance (*Rabus and Lang*, 2002), leading to a wider grounding zone for a given ice thickness compared to the simple beam model.~~

~~Over a straight section of the Carlson Inlet (cross-section A) the ice thickness at point H is 1081 m, which corresponds to a modelled grounding width of 4788 m. The ice thickness here is overestimated by 30% compared to the measured width of 3210 m (or 3260 m using DInSAR). This discrepancy is larger than over the straight section of the Evans Ice Steam (profile C in Figures 3 and 4), suggesting that either the ice is thinner, or the elastic modulus of the ice is lower. Areas of high stress in fast-flowing areas caused by localised high friction regions of the bed or side drag at the margins of the ice streams could cause fracturing or alter the ice fabric making it weaker. This could potentially be why there is 10% overestimation of the elastic beam model over the Evans Ice Steam. However the ice is effectively stagnant over the Carlson Inlet, so this difference is probably due to an underestimation of ice thickness using the assumption of hydrostatic equilibrium or other unmodelled processes.~~

~~Fracturing of the ice and the reduction of its effective thickness (relative to the modelled value) can also be caused by the motion of the ice shelf due tides (*Hulbe et al.*, 2016; *Rosier et al.*, 2017). If we compare the relationship of grounding line width of a simple elastic beam for areas of a large tidal range (>1 m) and small tidal range (<1 m) we find $X = (24.5 \pm 6.2)h^{3/4}$ and $X = (27.6 \pm 6.2)h^{3/4}$ respectively, suggesting the ice is weaker for higher tidal ranges.~~

Other models that include 2-D flexure of the ice shelf (*Schmeltz et al.*, 2002; *Marsh et al.*, 2014) or modelling ice as a viscoelastic material (*Wild et al.*, 2018) would provide a more accurate representation of the grounding zone. However,

a ~~more~~ sophisticated model is beyond the scope of the present study, and ~~without including other factors that determine grounding zonewidth, we can only qualitatively asses the differences in ice thickness observed~~the data is too noisy to infer any further information about the structure of the grounding zone. Nevertheless, the effective Young's modulus calculated here of $E = 1.4 \pm 0.9$ GPa, agrees well with previous calculations of $E = 0.88 \pm 0.35$ GPa, $E = 1.1$ GPa and $E = 9$ GPa by *Vaughan* (1995), *Smith* (1991) and *Stephenson* (1984) respectively; while other modelling studies have found the range between $E = 0.8$ and 3.5 GPa (*Schmeltz et al.*, 2002) and $E = 1.4 \pm 0.35$ (*Marsh et al.*, 2014).

7 Conclusions

We used 7.5 years of CryoSat-2 SARIn POCA and swath data to map points F and H of the Antarctic grounding zone. We managed to obtain near-complete coverage of the grounding zones of the Siple Coast region of the Ross Ice Shelf and Filchner-Ronne Ice Shelf. However, in lower latitude areas, further north, coverage is variable. Where the tidal range is small and swath data was the primary data source for resolving the tidal signal (e.g. the ~~Admunsen Sea sector~~Amundsen Sea Sector) we lose coverage, while in areas with a larger tidal range such as Dronning Maud ~~land~~ Land and the Larsen Ice Shelf, we were able to map a significant proportion of the grounding zone. The mapped point F compared well to previous methods with a negligible bias of -0.1 km and -0.1 km and a standard deviation of 1.1 km and 1.5 km between DInSAR and ICESat measurements, respectively. Over these regions we observed no significant deviation between previously mapped point F, as these regions are known to be relatively stable with no significant grounding zone retreat previously recorded, and our results support this. For the Support Force Glacier and the Doake Ice Rumples of the Filchner-Ronne Ice Shelf, we mapped regions that were previously only mapped using break-in-slope methods.

The results of mapping points F and H ~~were then used to investigate~~ investigated the spatial distribution of the grounding zone width, ~~X~~W, across Antarctica ~~. This allowed us to investigate~~ allowing us to examine the grounding zone structure across a significant fraction of the Antarctic coastline. ~~X~~ W showed a strong regional variation, and to a first approximation, the grounding line width is dependent on ice thickness. Relating our results to an elastic beam model of the grounding zone and ice shelf thickness measurements, we ~~found $X = (25.4 \pm 0.3)h^{3/4}$~~calculated the effective Young's modulus of $E = 1.4 \pm 0.9$ GPa, which compares well to previous studies. ~~There was considerable scatter in the fit, however,~~ However we could not infer any further infomation about the structure of the grounding zone as there are measurement errors in both ice shelf thickness and grounding zone width, as well as un-modelled factors ~~(~~such as grounding zone shape and ice rheology~~). For example over the Carlson Inlet and Evans Ice Stream, the simple beam model grounding line widths derived from ice shelf thickness showed significant deviations from the measured grounding line width using both CroySat-2 and DinSAR. Without the use of a more complex model of the grounding zone we could only qualitatively investigate potential factors which caused these deviations.~~

~~In areas where the grounding line has significantly retreated (e.g. the Amundsen Sea sector), the coverage was too sparse to detect any change. However, in areas where we were able to map a continuous grounding line, this method has the potential to monitor grounding line retreat and change in its structure, throughout the lifetime of the CryoSat-2 satellite.~~

Data availability. The data sets generated during this study are available at https://doi.org/10.5285/40c0b0c6-533c-43e7-9761-38225dac3084.

Author contributions. GJD undertook the data analysis developed the methods and wrote the paper. JLB conceived the study and both authors commented on the manuscript.

Competing interests. The authors declare no competing interest

Acknowledgements. This work was supported by the UK Natural Environment Research Council (NERC) grant NE/N011511/1. The European Space Agency (ESA) provided the CryoSat-2 data used for this research. We thank L. Gray for his advice in processing the CryoSat-2 swath data.

References

Bamber, J. L. and Bentley, C. R. A comparison of satellite-altimetry and ice-thickness measurements of the Ross Ice Shelf, Antarctica, Annals of Glaciology, 20, 357–364, https://doi.org/10.3189/1994AoG20-1-357-364, 1994.

Bamber, J. L., Gomez-Dans, J. L., and Griggs, J. A. A new 1 km digital elevation model of the Antarctic derived from combined satellite radar and laser data - Part 1: Data and methods, The Cryosphere 3, 101–111, https://doi.org/10.5194/tc-3-101-2009, 2009.

Bindschadler, R., Choi, H., Wichlacz, A., Bingham R. G., Bohlander J., Brunt K. M., Corr H., Drews R., Fricker H. A., Hall M. and others. Getting around Antarctica: new high-resolution mappings of the grounded and freely-floating boundaries of the Antarctic ice sheet created for the International Polar Year. The Cryosphere 5, 569–588, https://doi.org/10.5194/tc-5-569-2011, 2011.

Bohlander, J., and Scambos T. A. Antarctic coastlines and grounding line derived from MODIS Mosaic of Antarctica (MOA), Boulder, Colorado USA: National Snow and Ice Data Center, 2007

Brunt, K. M., Fricker H. A, Padman L., Scambos T. A., and O'Neel S. Mapping the grounding zone of the Ross Ice Shelf, Antarctica, using ICESat laser altimetry, Annals of Glaciology, 51, 71–79, https://doi.org/10.3189/172756410791392790, 2010a.

Brunt, K. M., Fricker H. A., Padman L., and. O'Neel S. ICESat-Derived Grounding Zone for Antarctic Ice Shelves, Boulder, Colorado USA: National Snow and Ice Data Center. 2010b.

Chen, C. W. and Zebker, H. A. Two-dimensional phase unwrapping with use of statistical models for cost functions in nonlinear optimization. JOSA A, 18(2), 338-351, https://doi.org/10.1364/JOSAA.18.000338, 2001.

~~. (2001). Two-dimensional phase unwrapping with use of statistical models for cost functions in nonlinear optimization. JOSA A, 18(2), 338-351.~~

Christie, F. D. W., Bingham R. G., Gourmelen N., Tett S. F. and Muto A. Four-decade record of pervasive grounding line retreat along the Bellingshausen margin of West Antarctica. Geophysical Research Letters, 43, 5741–5749, https://doi.org/10.1002/2016GL068972, 2016.

Chuter, S. J. and Bamber, J. L. Antarctic ice shelf thickness from CryoSat-2 radar altimetry, Geophysical Research Letters, 42, 721–729, https://doi.org/10.1002/2015GL066515, 2015.

ESA Antarctic Ice Sheet Climate Change Initiative. Grounding Line Locations for the Ross and Byrd Glaciers, Antarctica, 2011-2017, v1.0. Centre for Environmental Data Analysis, 2017.

Dawson G. J. and Bamber J. L. Antarctic Grounding Line Mapping From CryoSat-2 Radar Altimetry, Geophysical Research Letters 44, 11,886-11,893, https://doi.org/10.1002/2017GL075589, 2017.

Depoorter, M. A, Bamber J. L., Griggs J. A., Lenaerts J. T. M., Ligtenberg S. R. M., van den Broeke M. R. and Moholdt G. Calving fluxes and basal melt rates of Antarctic ice shelves, Nature, 502, 89-92, https://doi.org/10.1038/nature12567, 2013.

Fricker, H. A. and Padman L. Ice shelf grounding zone structure from ICESat laser altimetry, Geophysical Research Letters, 33, L15502, https://doi.org/10.1029/2006GL026907, 2006.

Fretwell, P., Pritchard, H. D., Vaughan, D. G., Bamber, J. L et al. Bedmap2: improved ice bed, surface and thickness datasets for Antarctica, The Cryosphere 7, L375–393, https://doi.org/10.5194/tc-7-375-2013, 2013.

Gourmelen, N., Goldberg, D.N., Snow, K., Henley, S.F., Bingham, R.G., Kimura, S., Hogg, A.E., Shepherd, A., Mouginot, J., Lenaerts, J.T. and Ligtenberg, S.R. Channelized melting drives thinning under a rapidly melting Antarctic ice shelf, Geophysical Research Letters 44, 9796–9804. https://doi.org/10.1002/2017GL074929.

Gray, L., N. Short, Bindschadler R., Joughin I., Padman L., Vornberger P. and Khananian A. RADARSAT interferometry for Antarctic grounding-zone mapping, Annals of Glaciology 34, 269–276, https://doi.org/10.3189/172756402781817879, 2002.

Gray, L., Burgess D., Copland L., Cullen R., Galin N., Hawley R. and Helm V. Interferometric swath processing of Cryosat data for glacial ice topography, The Cryosphere, 7, 1857–1867, https://doi.org/10.5194/tc-7-1857-2013, 2013.

Gray, L.,. Burgess D, Copland L., Dunse T., Langley K. and Moholdt G. A revised calibration of the interferometric mode of the CryoSat-2 radar altimeter improves ice height and height change measurements in western Greenland, The Cryosphere 11, 1041–1058, https://doi.org/10.5194/tc-11-1041-2017, 2017.

Helm, V., Humbert A., and Miller H. Elevation and elevation change of Greenland and Antarctica derived from CryoSat-2. The Cryosphere, 8, 1539–1559, https://doi.org/10.5194/tc-8-1539-2014, 2014.

Hogg, A. E. and Shepherd A., Gilbert L., Muir A. and Drinkwater M. R. Mapping ice sheet grounding lines with CryoSat-2, Advances in Space Research, https://doi.org/10.1016/j.asr.2017.03.008, 2017

Holdsworth, G. Tidal interaction with ice shelves, Ann. Geophys. 33, 133–146, 1977

Howat, I. M., Porter, C., Smith, B. E., Noh, M.-J., and Morin, P. The Reference Elevation Model of Antarctica, The Cryosphere, 13, 665-674, https://doi.org/10.5194/tc-13-665-2019, 2019.

Jensen, J. R. Angle measurement with a phase monopulse radar altimete, IEEE Transactions on Antennas and Propagation, 47m 715–724, https://doi.org/10.1109/8.768812, 1999.

Hulbe, C. L., Klinger M., Masterson M., Catania G., Cruikshank K. and Bugni A Tidal bending and strand cracks at the Kamb Ice Stream grounding line, West Antarctica, Journal of Glaciology, 235, 816-–824, https://doi.org/10.1017/jog.2016.74, 2016.

Marsh, O. J. ,Rack W., Golledge N. R., Lawson W. and Floricioiu D. Grounding-zone ice thickness from InSAR: Inverse modelling of tidal elastic bending, Journal of Glaciology, 60, 526–536, https://doi.org/10.3189/2014JoG13J033, 2014.

McMillan, M., Shepherd A., Sundal A., Briggs K., Muir A., Ridout A., Hogg A. and Wingham D. Increased ice losses from Antarctica detected by CryoSat-2, Geophysical Research Letters, 41, 3899–3905, https://doi.org/10.1002/2014GL060111, 2014.

Moholdt, G., Padman, L. and Fricker, H. A. Basal mass budget of Ross and Filchner-Ronne ice shelves, Antarctica, derived from Lagrangian analysis of ICESat altimetry, Journal of Geophysical Research: Earth Surface 119, 2361–2380, https://doi.org/10.1002/2014JF003171, 2014.

Padman, L., Fricker H. A., Coleman R., Howard S. and Erofeeva L. A new tide model for the Antarctic ice shelves and seas, Annals of Glaciology, 34, 247–254, https://doi.org/10.3189/172756402781817752, 2002.

Rabus, B. T. and Lang, O. On the representation of ice-shelf grounding zones in SAR interferograms, Journal of Glaciology, 48, 345–356, https://doi.org/10.3189/172756502781831197, 2002.

Raney, R K. The delay/Doppler radar altimeter, IEEE Transactions on Geoscience and Remote Sensing, 36, 1578–1588, https://doi.org/10.1109/36.718861, 1998.

Rignot, E. Hinge-line migration of Petermann Gletscher, north Greenland, detected using satellite-radar interferometry, Journal of Glaciology, 44, 469–476, https://doi.org/10.3189/S0022143000001994, 1998.

Rignot, E., Mouginot J. and Scheuchl B. MEaSUREs InSAR-based Antarctica ice velocity map. Boulder, Colorado USA: NASA DAAC at the National Snow and Ice Data Center.2011

Rignot, E., Mouginot J.and Scheuchl B. Antarctic grounding line mapping from differential satellite radar interferometry, Geophysical Research Letters, 38, L10504, https://doi.org/10.1029/2011GL047109, 2011.

Rignot, E., Mouginot J., Morlighem M., Seroussi H. and Scheuchl B. Widespread, rapid grounding line retreat of Pine Island, Thwaites, Smith, and Kohler glaciers, West Antarctica, from 1992 to 2011, Geophysical Research Letters, 41, 3502–3509, https://doi.org/10.1002/2014GL060140, 2014.

Rignot, E., Mouginot J. and Scheuchl B. MEaSUREs Antarctic Grounding Line from Differential Satellite Radar Interferometry, Version 2. Boulder, Colorado USA. NASA National Snow and Ice Data Center Distributed Active Archive Center. Accessed on 4 September 2016.

Rosier, S H. R. and Marsh, O. J., Rack, W., Gudmundsson, G. H., Wild, C. T. and Ryan, M. On the interpretation of ice-shelf flexure measurements, Journal of Glaciology, 241, 783-–791, https://doi.org/10.1017/jog.2017.44, 2017.

Scheuchl, B. J. Mouginot J., Rignot E., Morlighem M. and Khazendar A. Grounding line retreat of Pope, Smith, and Kohler Glaciers, West Antarctica, measured with Sentinel-1a radar interferometry data, Geophysical Research Letters, 43, 8572–8579, https://doi.org/10.1002/2016GL069287, 2016.

Shepherd, A., Wingham D. J. and Mansley J. A. D. Inland thinning of the Amundsen Sea ~~sector~~Sector, West Antarctica, Geophysical Research Letters, 29, 2-2–2-4, https://doi.org/10.1029/2001GL014183, 2002.

Schmeltz, M., Rignot E., and Douglas M. Tidal flexure along ice-sheet margins: comparison of InSAR with an elastic-plate model, Annals of Glaciology, 34, 202–208, https://doi.org/10.3189/172756402781818049, 2002.

Smith A. The use of tiltmeters to study the dynamics of Antarctic ice-shelf grounding lines. Journal of Glaciology, 37(125), 51-58. doi:10.3189/S0022143000042799

Stephenson, S. N. Glacier Flexure and the Position of Grounding Lines: Measurements By Tiltmeter on Rutford Ice Stream, Antarctica, Annals of Glaciology, 5, 165–169, https://doi.org/10.3189/1984AoG5-1-165-169, 1984.

Sykes, H. .J and Murray, T. and Luckman, A. The location of the grounding zone of Evans Ice Stream, Antarctica, investigated using SAR interferometry and modelling, Annals of Glaciology 50, 35–40, https://doi.org/10.3189/172756409789624292, 2009.

Vaughan, D. Tidal flexure at ice shelf margins, Journal of Geophysical Research, 100, 6213–6224, https://doi.org/10.1029/94JB02467, 1995.

Wang, F., Bamber J. L. and Cheng X. Accuracy and performance of CryoSat-2 SARIn mode data over Antarctica, IEEE Geoscience and Remote Sensing Letters, 12, 1516–1520, https://doi.org/10.1109/LGRS.2015.2411434, 2015.

Wouters, B.,Martin-Español A. , Helm V., Flament T., van Wessem J. M., Ligtenberg S. R. M., van den Broeke M. R, and Bamber J. L. Dynamic thinning of glaciers on the Southern Antarctic Peninsula, Science, 348, 899–903, 10.1126/science.aaa5727, 2015

Wild, C. T., Marsh O. J. and Rack. W. Unraveling InSAR Observed Antarctic Ice-Shelf Flexure Using 2-D Elastic and Viscoelastic Modeling, Frontiers in Earth Science, 6, 28, https://doi.org/10.3389/feart.2018.00028, 2018.

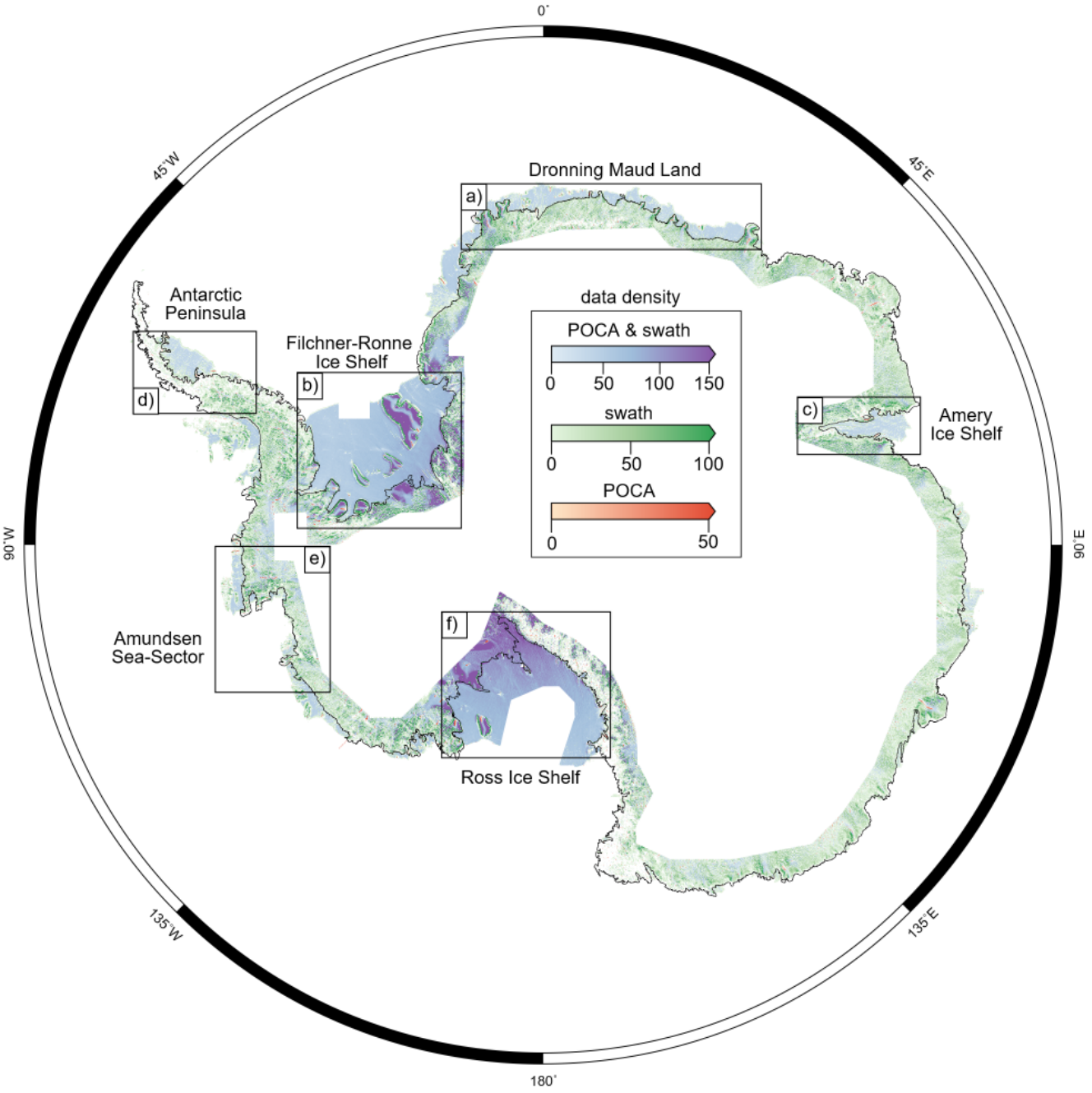

Figure 1. Data coverage plot for POCA and swath data. Red, green and blue data points correspond to where we used POCA, swath or both to calculate the tidal amplitude, T_d, respectively. The colour scales show the data density (POCA points/km). The swath data density is scaled by 150 (the average number of swath to POCA data points) to match the POCA density. The black line is a composite grounding line by *Depoorter et al.* (2013)

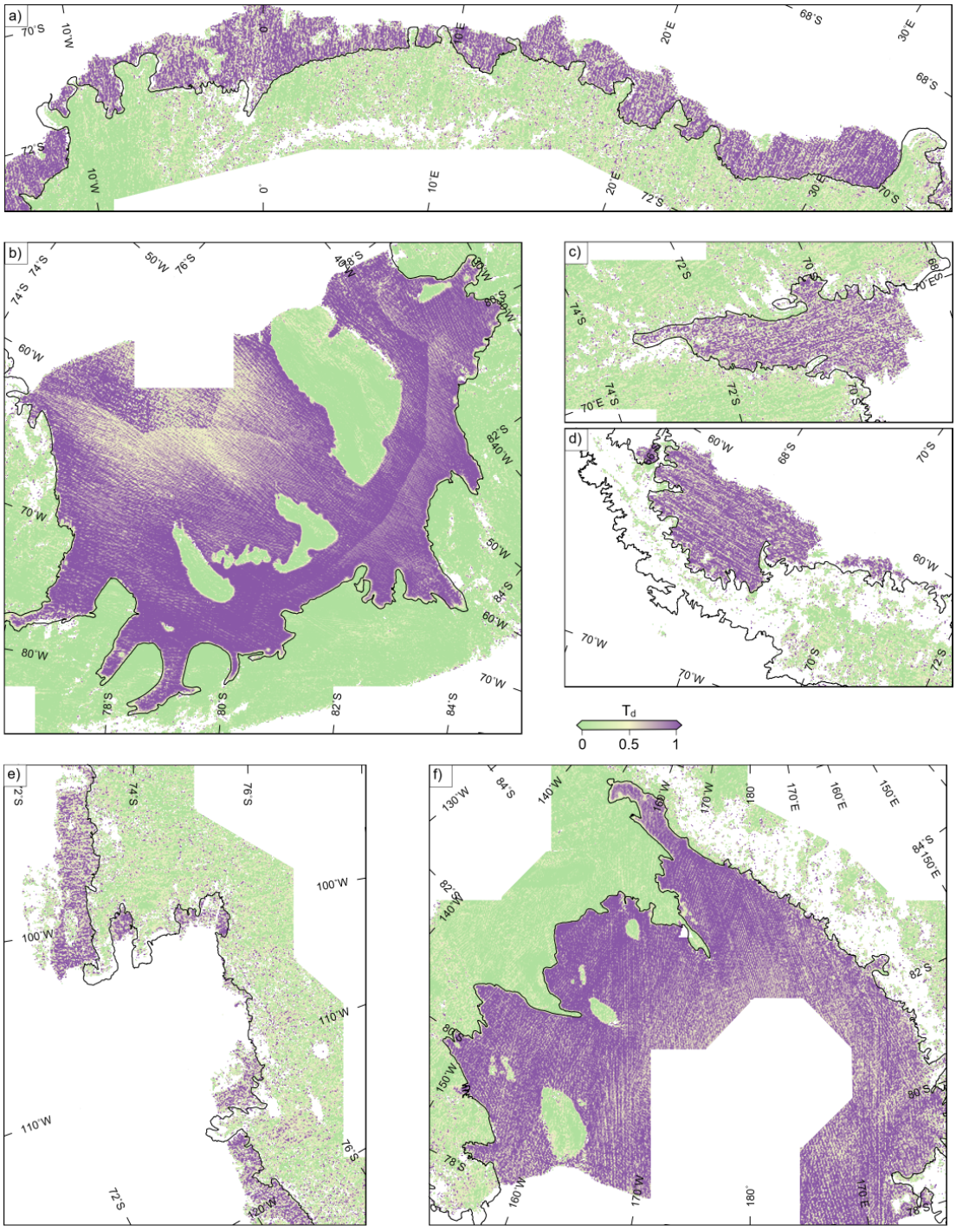

Figure 2. The dimensionless tidal amplitude ,T_d for a) Dronning Maud Land, b) Filchner-Ronne Ice Shelf, c) Amery Ice Shelf, d) Antarctic Peninsula. e) Amundsen Sea Sector and f) Ross Ice Shelf. The black line is a composite grounding line by *Depoorter et al.* (2013).

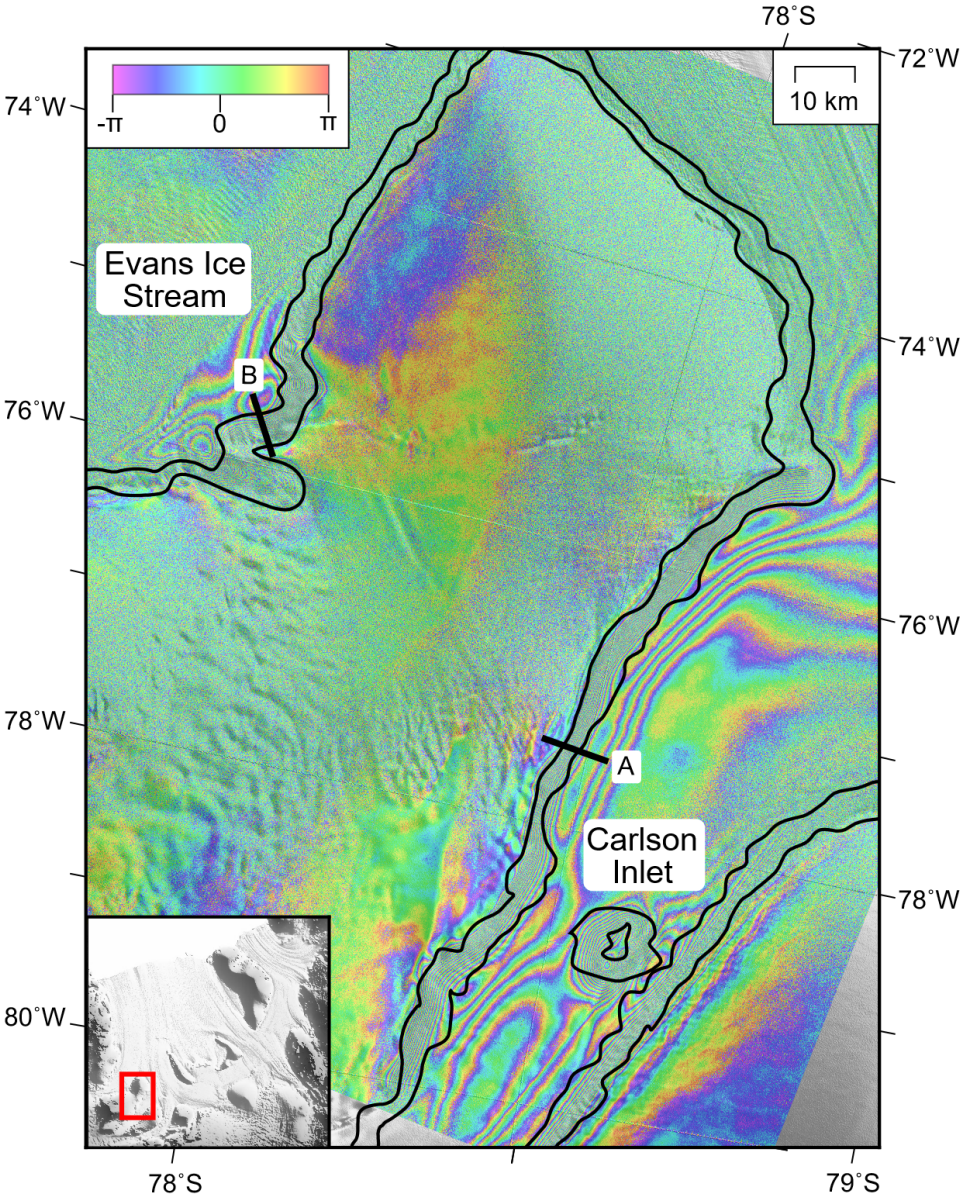

Figure 3. DInSAR interference fringes over the Evans Ice Stream and the Carlson Inlet of the Filchner-Ronne Ice Shelf, along with the CryoSat-2 mapped grounding line (points F and H, solid black lines), each fringe corresponds to 2.8 cm change in height due to the motion of tides.

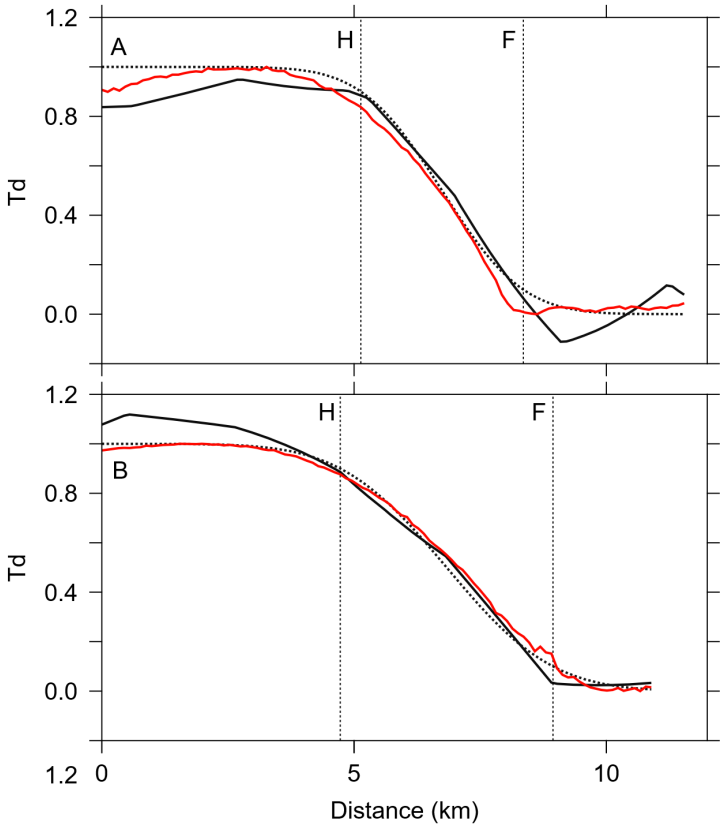

Figure 4. Cross-sections of T_d (solid black line) with the fitted error function (dashed black line) and the normalised deformation measured from Sentinel-1 double-differenced interferograms (red line), for ~~three~~ two cross-sections across the Carlson Inlet (A) and Evans Ice Stream (B~~and C~~) as shown in Figure 3.

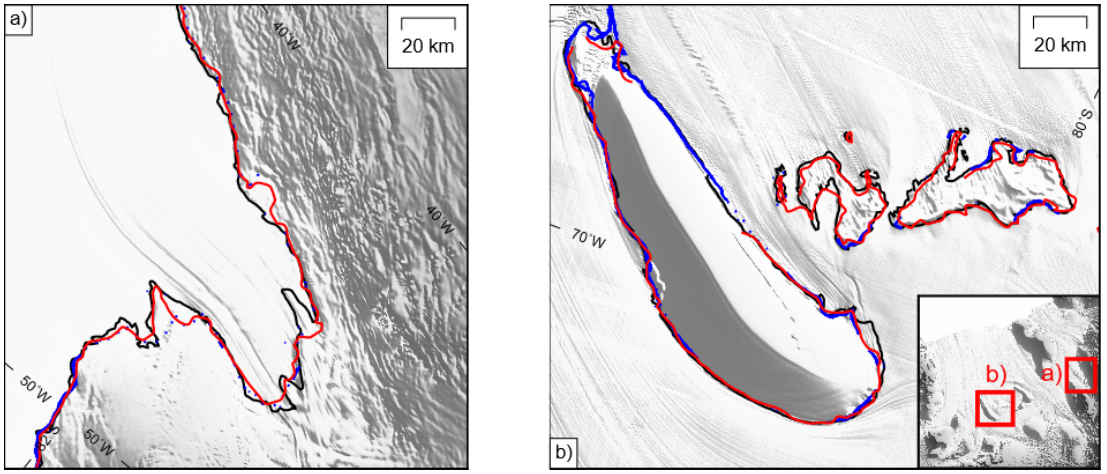

Figure 5. Grounding line ~~width, *W* for a~~mapped using DInSAR from both the MEaSUREs and the ESA CCI grounding line (blue)~~Dronning Maud Land~~, ~~b~~break-in-slope from the ASAID project grounding line (*Bindschadler et al.*, 2011)) ~~Filchner-Ronne Ice Shelf, c~~(black) ~~Amery Ice Shelf, d~~and CryoSat-2 (red) ~~Antarctic Peninsula. e~~methods for a) ~~Amundsen Sea Sector~~ Support Force Glacier and ~~f~~b) ~~Ross~~ Doake Ice ~~Shelf~~Rumples. The background image is ~~the ice shelf thickness (*Chuter and Bamber*, 2015)~~ overlain on the ~~Bedemap2~~ REMA DEM ~~(*Fretwell et al.*, 2006) .~~ (*Howat et al.*, 2019)

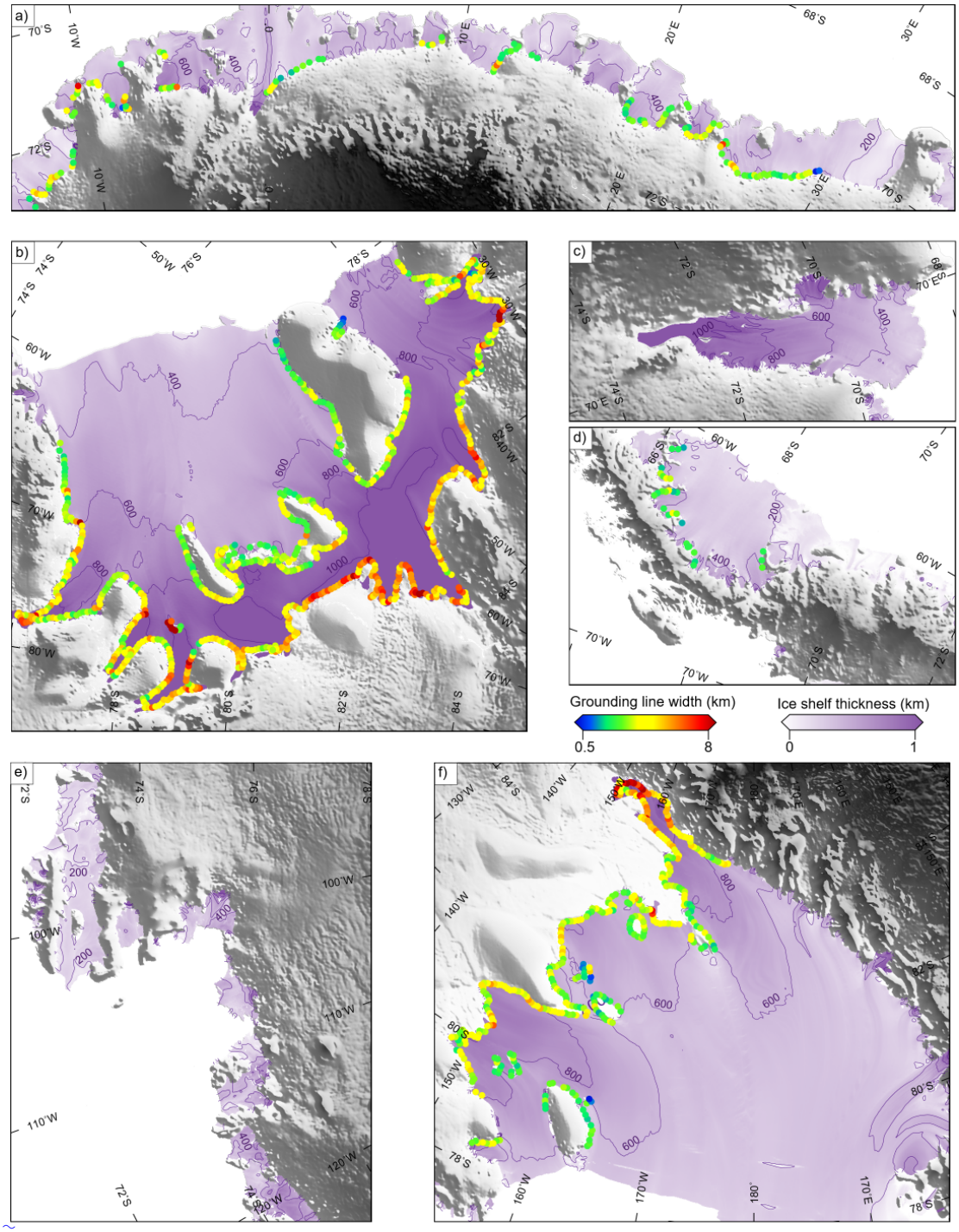

Figure 6. Grounding line width, *W* for a) Dronning Maud Land, b) Filchner-Ronne Ice Shelf, c) Amery Ice Shelf, d) Antarctic Peninsula. e) Amundsen Sea Sector and f) Ross Ice Shelf. The background image is the ice shelf thickness (*Chuter and Bamber*, 2015) overlain on the Bedmap-2 DEM (*Fretwell et al.*, 2006) .

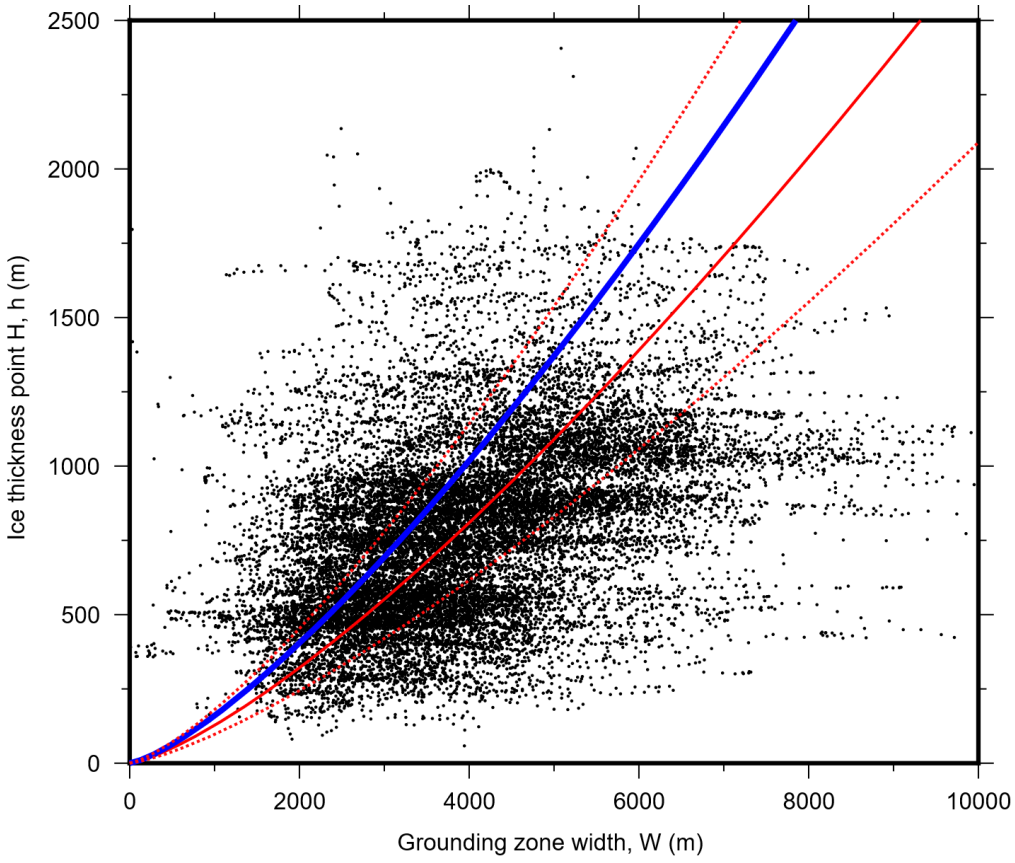

Figure 7. Grounding zone width (~~X~~W) vs ice thickness at point H (h). The solid red line is the fit of equation ~~$X = (26.4 \pm 6)h^{3/4}$~~ $W = (26.4 \pm 6)h^{3/4}$ to the data and the dashed red lines are the uncertainty bounds, ~~whi;c~~ while the blue line represents the estimation of *Vaughan* (1995) of ~~$X = (25.4 \pm 6.2)h^{3/4}$~~$W = (25.4 \pm 6.2)h^{3/4}$.

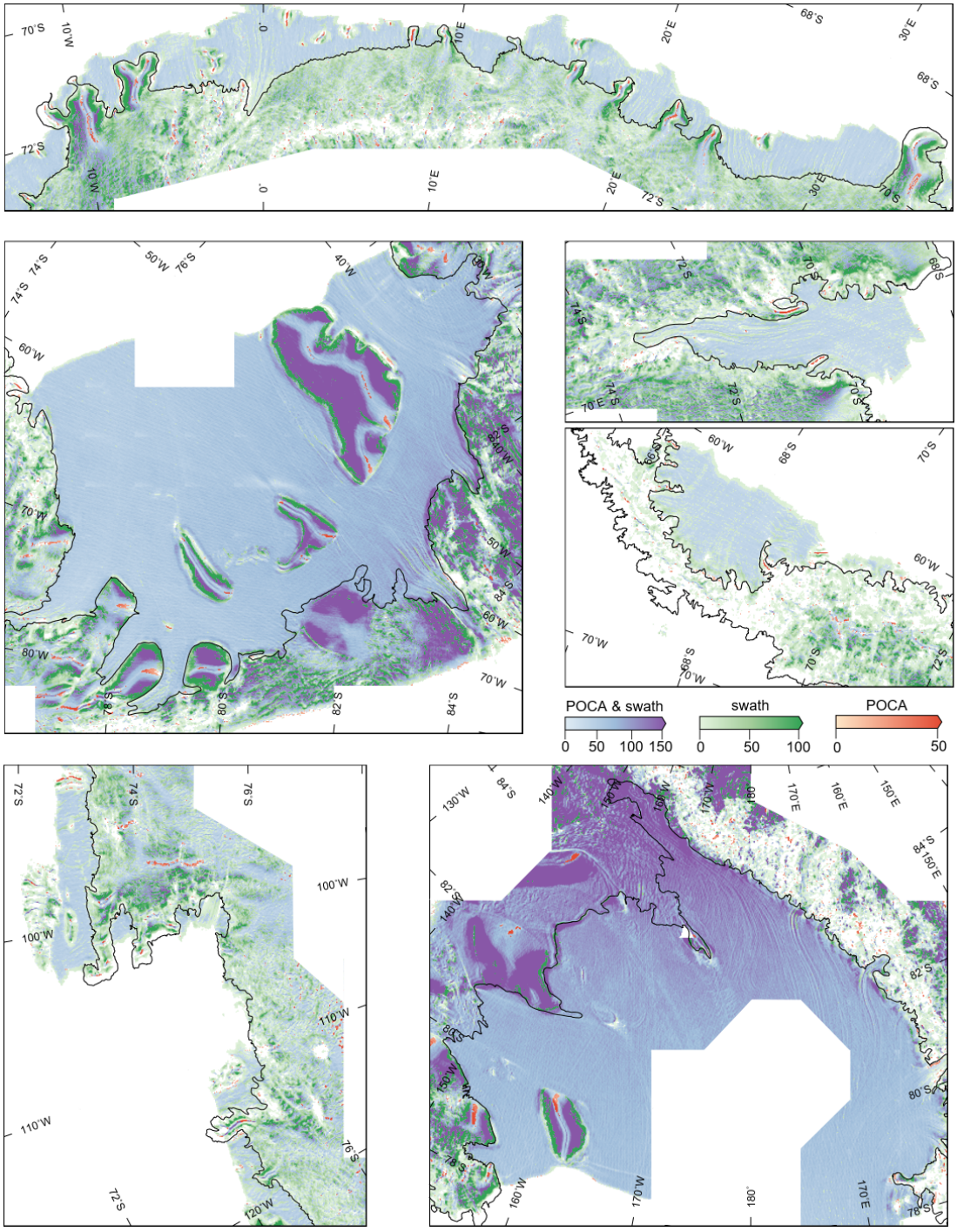

Figure A1. Data coverage plot for POCA and swath data. Red, green and blue data points correspond to where we used POCA, swath or both to calculate T_d, respectively. The colour scales shows the data density (POCA points/km). The swath data density is scaled by 150 (the average number of swath to POCA data points) to match the POCA density for a) Dronning Maud Land, b) Filchner-Ronne Ice Shelf, c) Amery Ice Shelf, d) Antarctic Peninsula. e) Amundsen Sea Sector and f) Ross Ice Shelf. The black line is a composite grounding line by *Depoorter et al.* (2013).

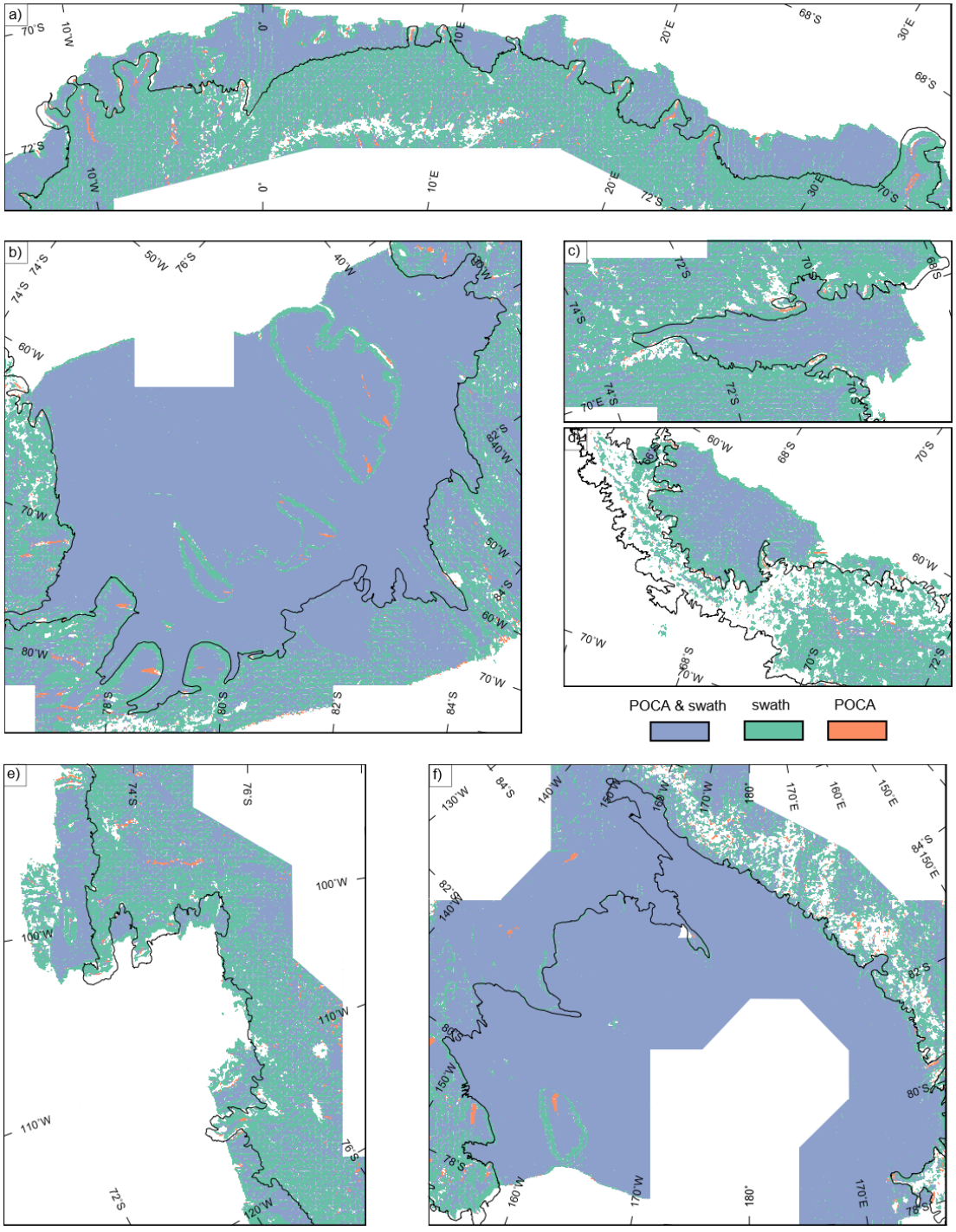

Figure A2. Data coverage plot for POCA and swath data. Purple, green and orange data points correspond to where we used POCA, swath or both to calculate T_d, respectively for a) Dronning Maud Land, b) Filchner-Ronne Ice Shelf, c) Amery Ice Shelf, d) Antarctic Peninsula, e) Amundsen Sea Sector and f) Ross Ice Shelf. The black line is a composite grounding line by *Depoorter et al.* (2013).

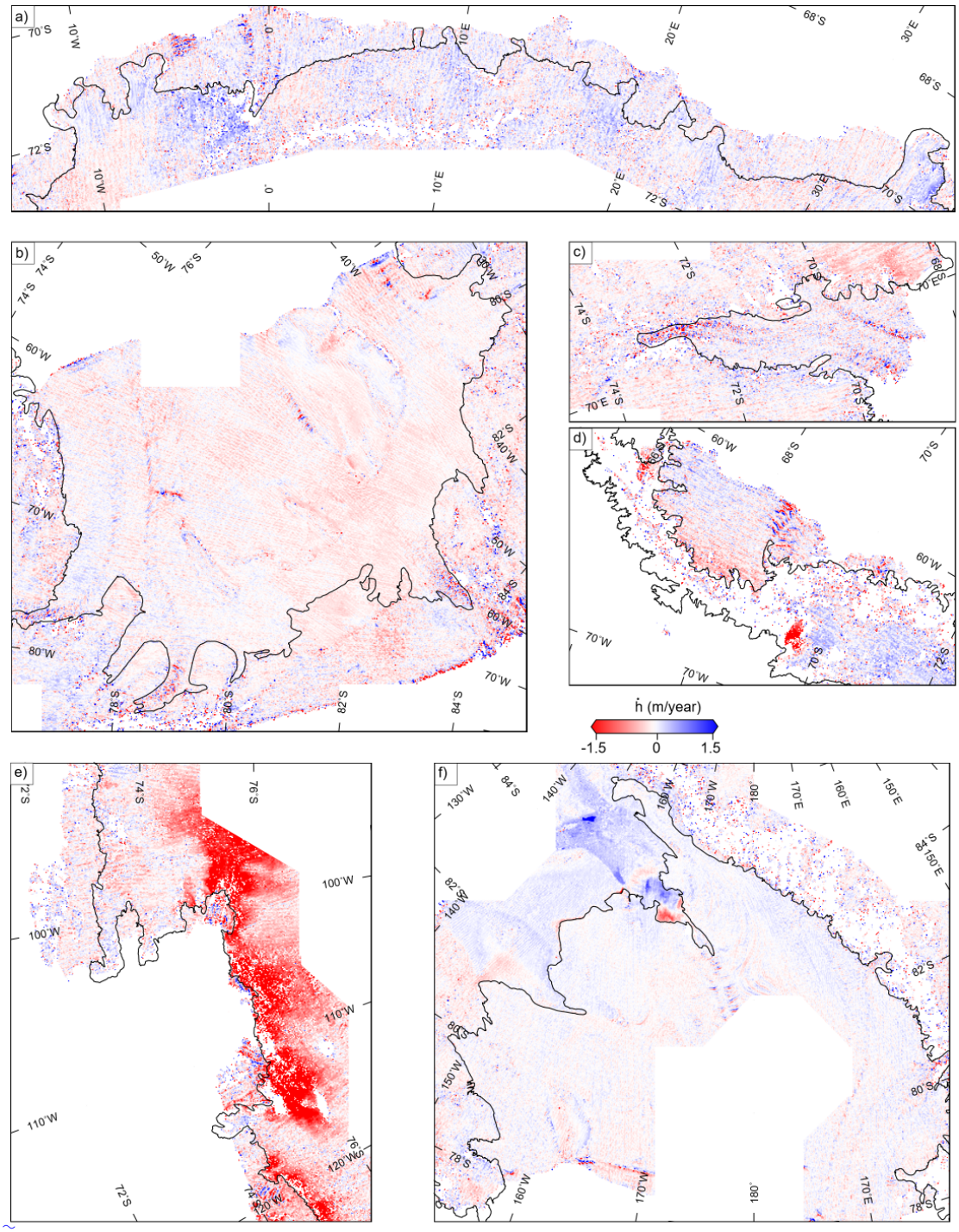

Figure A3. Elevation change ($\dot{h}$) for a) Dronning Maud Land, b) Filchner-Ronne Ice Shelf, c) Amery Ice Shelf, d) Antarctic Peninsula. e) Amundsen Sea Sector and f) Ross Ice Shelf.

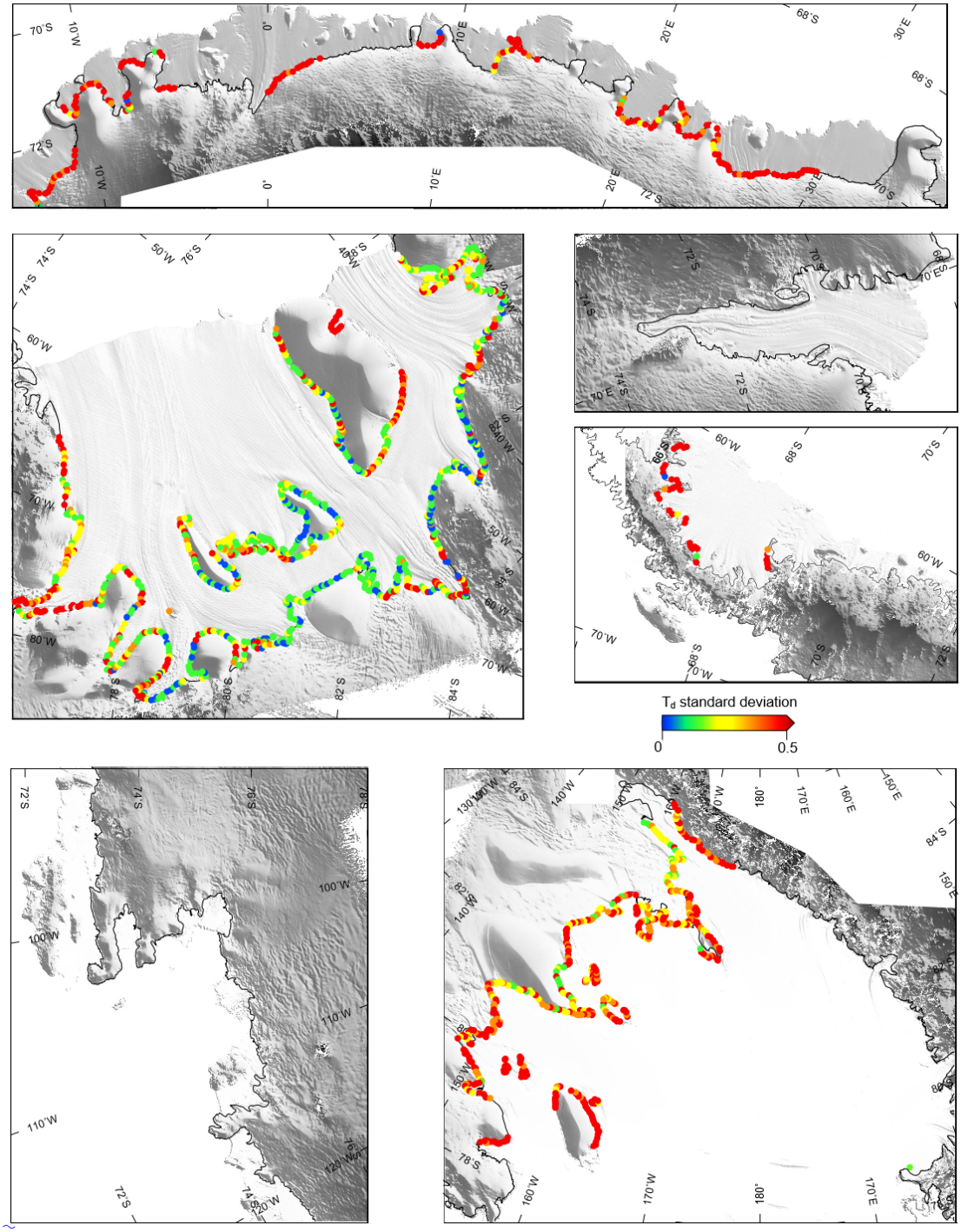

Figure A4. The satadardievaiton of T_d for the mapped grounding zone for a) Dronning Maud Land, b) Filchner-Ronne Ice Shelf, c) Amery Ice Shelf, d) Antarctic Peninsula. e) Amundsen Sea Sector and f) Ross Ice Shelf.